Finanziato dall'Unione europea NextGenerationEU | Ministero dell'Università e della Ricerca | Italiadomani PIANO NAZIONALE DI RIPRESA E RESILIENZA

multi-Risk sciEnce for resilienT commUnities undeR a changiNg climate Codice progetto MUR: **PE00000005** – E63C22002000002


# Deliverable title: Multi-criteria optimal selection of integrated mitigation/adaptation strategies for loss reduction

**Deliverable ID: 3.7.3**

**Due date:31/03/2026**

**Submission date: 31/03/2026**

**AUTHORS**

**Sara Alfano (UNIGE), Fabio Biondini (POLIMI), Martina Bosone (UNINA), Serena Cattari (UNIGE), Piero Colajanni (UNIPA), Jennifer D'Anna (UNIPA), Daniela Degregorio (UNINA), Pasquale De Toro (UNINA), Abbas FathiAzar (UNIGE), Maria Teresa Girardi (UNINA), Leila Jafari (POLIMI), Lidia La Mendola (UNIPA), Mattia Leone (UNINA), Simona Mancini (UNIPA), Stefano Nardone (UNINA), Giovanni Nocerino (UNINA), Alice Pallotta (UNINA), Roberto Paolucci (POLIMI), Francesca Linda Perelli (UNINA), Lorenza Petrini (POLIMI), Giulio Zuccaro (UNINA)**

# Technical references

| | |
|---|---|
| Project Acronym | RETURN |
| Project Title | multi-Risk sciEnce for resilienT commUnities undeR a changiNg climate |
| Project Coordinator | Domenico Calcaterra<br>UNIVERSITA DEGLI STUDI DI NAPOLI FEDERICO II<br>domcalca@unina.it |
| Project Duration | December 2022 – November 2025 (36 months) |

| | |
|---|---|
| Deliverable No. | DV 3.7.3 |
| Dissemination level* | PU |
| Work Package | WP3.7 - Strategies for loss reduction based on a systemic approach |
| Task | T3.7.3 - Multi-criteria optimal selection of integrated mitigation/adaptation strategies for loss reduction |
| Lead beneficiary | UNINA, M. Bosone, D. Degregorio, P. De Toro, M. T. Girardi, M. Leone, S. Nardone G. Nocerino A. Pallotta, L. Perelli, G. Zuccaro |
| Contributing beneficiary/ies | POLIMI, L. Jafari, F. Biondini, R. Paolucci, L. Petrini<br>UNIGE, S. Alfano, S. Cattari, A. FathiAzar<br>UNIPA, P. Colajanni, J. D'Anna; L. La Mendola S. Mancini |

* PU = Public

PP = Restricted to other programme participants (including the Ministry Services)

RE = Restricted to a group specified by the consortium (including the Ministry Services)

CO = Confidential, only for members of the consortium (including the Ministry Services)

# Document history

| Version | Date | Lead contributor | Description |
|---|---|---|---|
| 0.1 | xx.xx.xxxx | First name Last name<br><br>(Partner short name) | First draft |
| 0.2 | | | Critical review and proofreading |
| 0.3 | | | Edits for approval |
| 1.0 | | | Final version |

# ABSTRACT

Task 3.7.3 aimed to propose innovative concepts of adaptation/mitigation policy based on multi-objective and multi-criteria solutions to support decision-makers for optimal and sustainable loss prevention strategies across different spatial and operational scales.

First, the use of multi-criteria decision-making techniques by translating indicator-based resilience assessment frameworks into operational tools for strategy selection is proposed. Building on the Essential Resilience Indicators (ERI) system, indicators are structured, weighted, and linked to specific action domains, enabling their integration within a Multi-Criteria Decision Analysis (MCDA) framework. This approach allows for the evaluation and comparison of alternative strategies while explicitly considering trade-offs between effectiveness, cost, and long-term sustainability.

Second, a life-cycle-oriented, multi-objective prioritization framework is developed for bridge networks exposed to multiple hazards, including seismic events, flooding, and climate-induced deterioration processes. The methodology integrates probabilistic fragility models, network functionality indicators, recovery modelling, and socio-economic impact assessment. The results demonstrate that proactive adaptation and optimized intervention timing significantly enhance infrastructure resilience under evolving multi-hazard conditions.

Third, a two-stage stochastic optimization model is proposed to allocate resources between proactive strengthening and reactive repair in seismic regions. By incorporating uncertainty in damage scenarios and linking pre-event decisions with post-event outcomes, the model enables the minimization of expected evacuees under budget constraints. The application to a real case study shows that optimized allocation strategies outperform purely reactive approaches and that the balance between preventive and reactive measures depends on the relationship between damage levels and social impacts.

Finally, a multilevel optimization framework is developed for school building portfolios, integrating seismic safety, economic performance, and implementation constraints. The approach combines fragility-based assessment with evolutionary multi-objective optimization to identify cost-effective intervention strategies at portfolio scale. Results highlight the importance of prioritizing highly vulnerable buildings and underline the limited effectiveness of standalone energy retrofits, supporting the need for integrated seismic–energy strategies.

Overall, the deliverable demonstrates the potential of combining indicator-based frameworks, probabilistic modelling, and multi-objective optimization to support resilience-oriented decision-making. The proposed methodologies provide a coherent and scalable approach for addressing complex multi-risk challenges and contribute to the development of integrated strategies for disaster risk reduction and climate adaptation.

# 3. Table of contents

## List of Tables

## List of Figures

# 4. Development of multi- criteria techniques in the framework of selection of mitigation/adaptation strategies

## 4.1 Introduction

The increasing complexity of disaster risk in contemporary urban and territorial systems requires analytical and operational frameworks capable of addressing the interdependencies between multiple hazards, exposed elements and socio-economic dynamics. In recent decades, the growing frequency and intensity of climate-related events, combined with the persistent impact of geophysical hazards, have highlighted the limitations of traditional single-risk approaches and the need for integrated, multi-hazard perspectives. Within this context, international frameworks such as the IPCC reports and the Sendai Framework for Disaster Risk Reduction have progressively promoted a shift towards risk-based approaches, where risk is understood as the dynamic interaction between hazard, exposure and vulnerability within evolving socio-economic systems.

In parallel, resilience has emerged as a key concept for supporting disaster risk reduction and climate adaptation policies. Rather than focusing exclusively on the estimation of potential impacts, resilience-oriented approaches aim to capture the capacity of systems to cope with disturbances, adapt to changing conditions and transform in response to long-term challenges. However, despite the increasing availability of indicator-based frameworks for resilience assessment, a critical gap remains between the analytical phase and the operational dimension of decision-making. In particular, the translation of indicators into concrete actions and the selection of effective mitigation and adaptation strategies are often not explicitly addressed.

Within this framework, the work developed in Task 3.7.1 has focused on the construction of a structured indicator-based system for the assessment of disaster risk management practices and resilience conditions in urban and territorial contexts. Starting from a comprehensive review of international frameworks and best practices, a wide set of indicators has been defined, structured and progressively refined through expert-based evaluation processes. This process has led to the identification of a core subset of Essential Resilience Indicators (ERI), representing the most relevant variables for describing resilience conditions and supporting the comparison of alternative scenarios.

The methodological workflow adopted in this research follows a progressive logic of complexity reduction and operational enhancement. The initial phase is characterised by a broad and inclusive set of indicators, ensuring the representation of all relevant dimensions of resilience. Subsequent phases introduce processes of classification, prioritisation and weighting, leading to the definition of a reduced and structured set of indicators that can be effectively used within a multi-criteria evaluation framework. Through the application of the Simos “Pack of Cards” method, expert judgement and stakeholder perspectives are integrated into a consistent weighting system, allowing the transformation of qualitative and quantitative information into shared resilience metrics.

Building upon these results, the present deliverable – developed within Task 3.7.3 – extends the methodological framework towards a decision-support perspective. In particular, it focuses on the translation of Essential Resilience Indicators into action domains and governance strategies, and on their integration within a Multi-Criteria Decision Analysis (MCDA) framework aimed at supporting the optimal selection of mitigation and adaptation strategies for loss reduction. In this perspective, indicators are no longer interpreted solely as descriptive variables, but become evaluation criteria within a structured decision-making process.

Furthermore, the proposed approach is fully integrated with the broader modelling framework developed within the project, in which resilience metrics are combined with scenario-based quantitative indicators derived from risk and impact models. This integration allows the analysis and comparison of alternative resilience scenarios, taking into account the dynamic evolution of exposure, vulnerability and governance conditions. The use of GIS-based tools and spatial analysis further enhances the operational value of the framework, enabling the visualisation and evaluation of the spatial effects of different strategies.

Overall, the research contributes to the development of a holistic and operational framework that bridges the gap between resilience assessment and strategy selection. By linking indicator-based analysis, resilience theory and multi-criteria decision methods, it provides a structured approach for supporting decision-makers in the definition of integrated, multi-objective and sustainable disaster risk reduction and climate adaptation strategies.

## 4.2 Methodological workflow

The VS3 framework introduces a set of key innovations that significantly enhance its operational value. In the first three methodological phases (described in DV 3.7.1) a first evaluation framework was developed – in collaboration with the Task 5.2.4 "Best practices for urban and metropolitan risk management" (Spoke 5 - TS1 "Urban and Metropolitan Settlements") – aimed at identify and assess good practices in disaster risk reduction. Then, the broad set of indicators defined in the original framework is refined through a relevance-based and expert-based selection process, leading to the identification of a subset of 'Essential Resilience Indicators' (ERI), specifically related to spoke's goals, that are most significant for resilience assessment. This step is essential to reduce complexity and to ensure that the resulting system can be effectively used within decision-support processes.

In the last two phases, here described, the research group of VS3 adopted a Multi-Criteria weighting method to determine the relative importance of each indicator based on expert judgement. Finally, the ERI framework is operationalised by establishing explicit links between each indicator and a set of potential actions, thereby creating a direct connection between the analytical dimension of resilience assessment and the operational dimension of strategy development. In this way, the overall structure is reorganised to facilitate its integration within scenario-based analyses and the comparison of alternative strategies.

### 4.2.1. Indicator weighting using the revised Simos' Pack of Cards method

Once the most relevant indicators have been identified through the classification process described in the previous chapter, it becomes necessary to determine their relative importance within the evaluation framework. Indeed, even among the indicators considered highly relevant, different variables may contribute in different ways to the overall assessment of resilience conditions.

The weighting procedure was carried out through the involvement of both internal project experts and external stakeholders with expertise in disaster risk management, urban planning and resilience policies.

This participatory approach allows the weighting process to integrate different types of knowledge, including scientific expertise, operational experience and policy perspectives. The combination of these viewpoints contributes to increasing the robustness and legitimacy of the resulting resilience metrics.

When multiple participants are involved in the evaluation process, the individual weight sets obtained through the Simos method can be aggregated using statistical procedures, such as averaging or consensus-based methods, in order to obtain a final set of weights representing the collective judgement of the group.

This process ensures that the resulting weighting scheme reflects a shared understanding of the relative importance of the indicators. Indicator weighting therefore represents a fundamental step in the development of resilience metrics. Assigning weights to indicators allows their relative contribution to be explicitly considered when combining them into synthetic metrics or evaluation indices.

Within multi-criteria evaluation frameworks, weighting procedures are typically used to translate expert judgement and stakeholder preferences into quantitative values that reflect the relative importance of each indicator. This process helps to ensure that the final evaluation framework reflects both scientific knowledge and practical experience related to disaster risk management.

For this purpose, the present research adopts the revised Simos "Pack of Cards" method (Figueira & Roy, 2002), a structured preference elicitation technique widely used in multi-criteria decision analysis.

The Simos method, originally proposed by Jean Simos and later refined by Figueira and Roy, is a participatory weighting technique designed to support the elicitation of preferences in multi-criteria decision-making

processes. The method is particularly suitable for situations where experts are asked to express their judgement regarding the relative importance of a set of criteria or indicators. The procedure is based on a simple and intuitive process in which each criterion or indicator is represented by a "card" and participants are asked to arrange the cards according to their perceived importance. The main advantage of the Simos method lies in its ability to transform qualitative rankings provided by experts into quantitative weights, while maintaining a transparent and participatory evaluation process. In addition, the method allows participants to express not only the order of importance between indicators but also the intensity of preference, which reflects how much more important one indicator is compared to another.

The application of the Simos method in this research follows a structured sequence of steps designed to capture expert preferences and derive consistent indicator weights.

First, each of the indicators selected during the relevance classification phase is represented by an individual card. These cards are then presented to the participating experts.

Second, participants are asked to rank the indicators from the least important to the most important, according to their perceived contribution to resilience assessment. Indicators considered equally important may be grouped together.

Third, participants are given a set of blank cards, which can be inserted between groups of indicators in order to express differences in importance between them. The number of blank cards inserted between two groups reflects the perceived distance in importance between those indicators.

Fourth, participants are asked to define the ratio between the most important and the least important indicators, which represents the maximum difference in importance within the evaluation framework.

Based on these elements – the ranking of indicators, the number of blank cards inserted between groups and the maximum importance ratio – it is possible to calculate a set of normalized weights for each indicator.

The resulting weights reflect the preferences expressed by the experts and can be used to aggregate the indicators within the resilience evaluation framework.

The final outcome of the weighting procedure is a set of normalized weights associated with each selected indicator. These weights quantify the relative contribution of the indicators within the resilience assessment framework (Table 1).

Table 1 - Weights resulting from the application of revised Simos' method to the ERI

| Criteria | Criteria Description | Criteria Weight | Sub-criteria ID | Sub-criteria Description | Local Sub-criteria Weights | Global Sub-criteria and Criteria Weights | Global Sub-criteria and Criteria Weights (%) |
|---|---|---|---|---|---|---|---|
| **A** | Exposure and Vulnerability | 0,125 | A1 | Exposure of the building stock | 0,188 | 0,024 | 2,35 |
| | | | A2 | Vulnerability of the building stock | 0,244 | 0,031 | 3,05 |
| | | | A3 | Exposure of green and open spaces | 0,259 | 0,032 | 3,24 |
| | | | A4 | Vulnerability of green and open spaces | 0,309 | 0,039 | 3,86 |
| | | | | | **1,000** | | |
| **B** | Hazards and Impacts | 0,132 | B1 | Climatic and geophysical hazards | 0,450 | 0,059 | 5,94 |
| | | | B2 | Climatic and geophysical impacts | 0,550 | 0,073 | 7,26 |
| | | | | | **1,000** | | |
| **C** | Practices validation and update | 0,127 | C1 | Validated tools for risk and impact assessment for relevant hazards | 0,137 | 0,017 | 1,74 |

| | | | | | | | |
|---|---|---|---|---|---|---|---|
| | | | C2 | Avalaibility of hazard maps for relevant risks in the city | 0,129 | 0,016 | 1,64 |
| | | | C3 | Avalaibility of impact maps for relevant risks in the city | 0,134 | 0,017 | 1,70 |
| | | | C4 | Disaster management plans for all relevant risks in the city | 0,157 | 0,020 | 1,99 |
| | | | C5 | Validated disaster management plans for all multi-risk scenarios | 0,186 | 0,024 | 2,36 |
| | | | C6 | Practice drills and emergency training exercises involving relevant organizations and communities | 0,257 | 0,033 | 3,26 |
| | | | | | **1,000** | | |
| **D** | System of stakeholders/policy makers | 0,154 | D1 | Stakeholders categories involved in DRR planning | 0,129 | 0,020 | 1,99 |
| | | | D2 | Formalized partnership with research organisations | 0,188 | 0,029 | 2,90 |
| | | | D3 | Database of structured volunteers organisation | 0,316 | 0,049 | 4,87 |
| | | | D4 | Database of the resources supported by volunteers | 0,367 | 0,057 | 5,65 |
| | | | | | **1,000** | | |
| **E** | Consideration of vulnerable groups within the development of DRR plans | 0,157 | | | | 0,157 | 15,70 |
| **F** | Public communication | 0,152 | F1 | Guidelines for practitioners to address DRR and CCA in planning and design activities | 0,153 | 0,023 | 2,33 |
| | | | F2 | Open-access webportal regarding DRR | 0,253 | 0,038 | 3,85 |
| | | | F3 | Instruments to assess population's risk perception | 0,219 | 0,033 | 3,33 |
| | | | F4 | Types of media channel used to alert people during the emergency | 0,201 | 0,031 | 3,06 |
| | | | F5 | Online or off-line communication materials produced in different languages used in the city | 0,174 | 0,026 | 2,64 |
| | | | | | | | |
| **G** | Economic measures stored/invested for public and private resilience | 0,153 | | | | 0,153 | 15,30 |
| | | **1,000** | | | | **1,000** | **100,00** |

The weighted indicators form the basis for the identification of the ERI and for the development of shared resilience metrics capable of supporting risk and resilience assessments.

By combining the selected indicators with their corresponding weights, it becomes possible to construct synthetic shared resilience metrics that can be used to analyse the resilience conditions of urban and

territorial systems, compare alternative resilience scenarios and to support decision-making processes related to disaster risk reduction and climate adaptation strategies.

### 4.2.2. From indicator-based assessment to action-oriented frameworks

The identification and weighting of the ERI represent a fundamental step in the development of shared resilience metrics; however, their full operational value emerges only when they are translated into concrete actions and decision-support strategies. As highlighted in the previous sections, a major limitation of many indicator-based frameworks lies in the gap between the analytical phase and the actual definition of mitigation and adaptation measures . In this perspective, the present phase addresses this gap by transforming the ERI system into an action-oriented framework capable of supporting the selection of integrated strategies for loss reduction.

This transition is fully coherent with the evolution of risk assessment approaches towards a risk-based and decision-oriented paradigm, in which resilience is not only measured but actively operationalised through planning and governance processes. In line with recent literature, and in particular with the framework proposed by Turchi et al. (2023), resilience is interpreted as the result of the interaction between coping, adaptive and transformative capacities, which reflect different temporal horizons and intervention logics. These dimensions provide the conceptual basis for structuring the link between indicators and actions, allowing each ERI to be interpreted not only as a descriptive variable but as a driver of specific types of interventions.

At the same time, this step ensures continuity with the broader project framework and with the objectives of Task 3.7.3, which aims to establish a new concept of mitigation and adaptation policy based on multi-objective and multi-criteria approaches. In this perspective, the ERI are integrated with scenario-based quantitative indicators derived from impact models, contributing to the construction of a comprehensive evaluation framework in which resilience conditions, risk scenarios and intervention strategies can be jointly analysed.

### 4.2.3. Identification of action domains and linkage with resilience capacities

The translation of ERI into actions is based on a reinterpretation of the indicator system according to the three core dimensions of resilience. This step allows the definition of coherent “action domains”, each corresponding to a specific type of intervention logic and governance scale.

Indicators associated with coping capacity are linked to short-term, reactive actions aimed at managing the immediate impacts of hazardous events. These include interventions related to emergency preparedness, early warning systems, operational coordination, and the availability of response resources. In this domain, actions are primarily focused on ensuring the continuity of critical functions and reducing the immediate consequences of extreme events. As highlighted in the literature, coping capacity represents the first line of defence against disasters, enabling systems to absorb shocks and maintain essential operations.

Indicators associated with adaptive capacity correspond to medium-term actions aimed at reducing vulnerability and improving system performance over time. These actions include spatial planning measures, infrastructure upgrading, environmental management strategies and the development of knowledge tools such as hazard and impact maps. In this case, the focus shifts from reaction to anticipation, emphasising the importance of learning processes, risk-informed planning and the progressive adjustment of urban systems to changing conditions.

Finally, indicators associated with transformative capacity are linked to long-term actions aimed at enabling systemic change. These include governance reforms, stakeholder engagement processes, participatory planning mechanisms and the strengthening of social capital. In this domain, resilience is interpreted as the ability to redefine development pathways, integrating disaster risk reduction, climate adaptation and broader sustainability objectives. As underlined in previous studies, transformative capacity plays a crucial role in bridging the gap between technical solutions and societal change, allowing resilience strategies to be embedded within institutional and social structures.

Through this classification, each ERI is associated with one or more types of actions, depending on its contribution to different resilience capacities. This approach allows the construction of a structured

relationship between indicators and interventions, in which the multidimensional nature of resilience is explicitly reflected in the diversity of action types.

### 4.2.4. From actions to governance strategy blocks

Building on the identification of action domains, the next step consists in grouping actions into coherent "strategy blocks" that can support decision-making processes within a multi-criteria framework. These blocks represent clusters of interventions characterised by similar objectives, temporal horizons and governance mechanisms.

Three main strategic blocks can be identified. The first corresponds to **response-oriented strategies**, which are primarily associated with coping capacity and include actions related to emergency management, alert systems and operational preparedness. These strategies are essential for reducing immediate losses and ensuring rapid response during crisis situations, but they generally have limited long-term effects if not integrated with broader planning measures.

The second block corresponds to **preventive and adaptive strategies**, which are associated with adaptive capacity and include interventions aimed at reducing exposure and vulnerability through planning, infrastructure and environmental management. These strategies operate over medium time horizons and play a key role in improving the overall performance of urban systems, contributing to the reduction of risk conditions before hazardous events occur.

The third block corresponds to **transformative and governance-oriented strategies**, which are linked to transformative capacity and include actions related to institutional innovation, stakeholder engagement, social inclusion and long-term investment policies. These strategies aim to address the root causes of vulnerability and to enable systemic change, supporting the transition towards more resilient and sustainable development pathways.

In addition to these three main blocks, it is important to recognise the existence of hybrid strategies that combine elements of different capacities. For example, actions related to communication systems or risk information platforms may simultaneously contribute to coping, adaptive and transformative capacities, highlighting the interconnected nature of resilience processes.

The translation of Essential Resilience Indicators into action domains and strategy blocks allows the operationalisation of the indicator-based framework within a decision-support perspective. As shown in Table 2, each indicator can be interpreted as a driver of specific actions, which can be grouped into coherent resilience strategies corresponding to coping, adaptive and transformative capacities.

Table 2 - Link between ERI, actions and strategies

| ERI (Criteria / Sub-criteria) | Resilience Capacity | Type of Actions | Strategy Block | Operational Interpretation |
|---|---|---|---|---|
| **A1–A4 Exposure & Vulnerability** | Adaptive | Vulnerability reduction measures, spatial planning, building retrofitting, ecosystem-based solutions | Preventive / Adaptive strategies | Reduce exposure and improve system performance over time |
| **B1 Hazards / B2 Impacts** | Coping + Adaptive | Risk and impact assessment, scenario modelling, integration of hazard knowledge into planning and emergency protocols | Hybrid (Response + Adaptation) | Support both emergency awareness and anticipatory planning |
| **C1–C3 Tools and maps** | Adaptive | Development of hazard and impact maps, risk assessment tools, data integration platforms | Knowledge-based adaptive strategies | Enable risk-informed decision-making and planning |
| **C4–C6 Plans and drills** | Coping + Adaptive | Emergency planning, multi-risk management plans, drills and training exercises | Response + Preventive strategies | Link preparedness with structured planning processes |
| **D1 Stakeholder involvement** | Transformative | Stakeholder inclusion in planning processes, governance coordination mechanisms | Transformative governance strategies | Strengthen institutional capacity and inclusiveness |
| **D2 Research partnerships** | Adaptive + Transformative | Science–policy integration, knowledge co-production, innovation processes | Innovation-oriented strategies | Bridge technical knowledge and governance transformation |

| | | | | |
|---|---|---|---|---|
| **D3–D4 Volunteers and resources** | Coping + Transformative | Mobilisation of volunteer networks, resource management systems | Response + Social resilience strategies | Enhance emergency capacity and long-term social capital |
| **E Vulnerable groups inclusion** | Adaptive + Transformative | Inclusive planning, equity-oriented DRR strategies, targeted support measures | Inclusive strategies | Address social vulnerability and ensure equitable resilience |
| **F1 Guidelines** | Adaptive | Development of technical guidelines for DRR/CCA integration in planning and design | Preventive strategies | Support consistent and risk-informed planning practices |
| **F2 Web portals** | Adaptive + Transformative | Open-access platforms for risk information, transparency tools | Knowledge & governance strategies | Improve accessibility of information and institutional transparency |
| **F3 Risk perception tools** | Transformative | Awareness campaigns, surveys, participatory tools | Transformative strategies | Enable behavioural change and social learning processes |
| **F4 Alert systems** | Coping | Early warning systems, emergency communication channels | Response strategies | Ensure timely and effective emergency response |
| **F5 Multilingual communication** | Coping + Adaptive + Transformative | Inclusive communication systems, accessibility of information | Cross-cutting strategies | Support response, adaptation and social inclusion simultaneously |
| **G Economic measures** | Adaptive + Transformative | Investment strategies, funding allocation, economic incentives for resilience | Strategic / long-term strategies | Enable structural change and long-term resilience pathways |

### 4.2.5. Integration within a multi-criteria decision-support framework

The final step of the methodology consists in integrating the identified strategy blocks within a Multi-Criteria Decision Analysis (MCDA) framework, in order to support the comparison and selection of alternative mitigation and adaptation strategies. In this phase, the ERI no longer act only as indicators of resilience conditions, but become evaluation criteria used to assess the performance of different strategies.

The weights assigned to each indicator through the Simos method are used to quantify their relative importance within the evaluation process. By combining these weights with the performance of each strategy with respect to the selected indicators, it becomes possible to calculate synthetic scores that reflect the contribution of different strategies to resilience enhancement and loss reduction. This process allows the explicit consideration of trade-offs between different objectives, such as short-term effectiveness, long-term sustainability and social inclusiveness.

Within this framework, the integration with scenario-based modelling tools plays a crucial role. As highlighted in Deliverable 3.7.2, GIS-based simulations and dynamic risk maps allow the evaluation of the impacts of different strategies under alternative future scenarios, including climate change and urban development trajectories. The combination of MCDA and spatial analysis enables a comprehensive assessment of strategies, taking into account both their effectiveness in reducing risk and their spatial distribution across the territory.

Furthermore, the use of GIS tools enhances the transparency and accessibility of the results, allowing decision-makers and stakeholders to visualise the effects of different strategies and to better understand their implications. This contributes to strengthening participatory processes and to promoting collaboration between different actors involved in urban risk management.

Overall, the proposed framework represents a significant advancement with respect to traditional indicator-based approaches. By linking indicators, actions, strategies and decision-support tools within a coherent methodological structure, it provides an operational tool for supporting the optimal selection of mitigation and adaptation strategies in complex multi-risk scenarios. In doing so, it directly addresses the objectives of Task 3.7.3, contributing to the development of integrated, multi-objective and sustainable strategies for disaster risk reduction and climate adaptation.

# 5. Conclusions

This deliverable has presented the methodological framework developed within Task 3.7.3 for the multi-criteria selection of integrated mitigation and adaptation strategies aimed at reducing losses in multi-risk urban and territorial contexts. Building upon the results of Task 3.7.1, the work has extended the indicator-based assessment framework towards a fully operational decision-support system, capable of linking resilience metrics with concrete actions and governance strategies.

A key contribution of the research lies in the transformation of the Essential Resilience Indicators from descriptive variables into operational drivers of intervention. Through the reinterpretation of the indicator system according to the three core dimensions of resilience – coping, adaptive and transformative capacity – it has been possible to establish a structured relationship between indicators, action domains and strategic blocks. This approach allows the multidimensional nature of resilience to be explicitly reflected in the design and evaluation of mitigation and adaptation strategies, taking into account different temporal horizons and governance scales.

The identification of action domains and their aggregation into coherent strategy blocks represents a crucial step in reducing the complexity of the intervention space while preserving the richness of the analytical framework. In particular, the distinction between response-oriented, preventive/adaptive and transformative strategies allows the different roles of short-term, medium-term and long-term interventions to be clearly articulated. At the same time, the recognition of hybrid and cross-cutting actions highlights the interconnected nature of resilience processes and the need for integrated approaches.

The integration of the proposed framework within a Multi-Criteria Decision Analysis approach further enhances its operational value. By combining weighted indicators with the performance of alternative strategies, the MCDA framework enables the explicit consideration of trade-offs between multiple objectives, such as effectiveness in reducing losses, long-term sustainability and social inclusiveness. This allows decision-makers to identify strategies that achieve a balanced combination of short-term and long-term benefits, supporting more informed and transparent decision-making processes.

An additional strength of the methodology lies in its integration with scenario-based risk modelling and spatial analysis tools. The combination of resilience metrics with quantitative indicators derived from impact models, together with the use of GIS-based simulations, allows the evaluation of strategies under different future scenarios, including those related to climate change and urban development. This integration provides a robust basis for assessing the effectiveness of interventions and for identifying priority areas for action.

From a broader perspective, the proposed framework contributes to advancing the state of the art in resilience assessment and disaster risk reduction by addressing one of the main limitations of traditional indicator-based approaches, namely the lack of explicit links with decision-making processes. By bridging the gap between analysis and action, the methodology supports the development of integrated, multi-objective and context-sensitive strategies, fully aligned with the principles of the IPCC risk-based approach and the Sendai Framework.

Finally, the flexibility and scalability of the framework make it applicable to different territorial contexts and hazard configurations. While some limitations remain, particularly related to data availability and the reliance on expert judgement in certain phases of the process, the overall approach provides a transparent, replicable and operational tool for supporting resilience planning and policy-making.

In conclusion, the work developed within Task 3.7.3 demonstrates how the integration of indicator-based assessment, resilience theory and multi-criteria decision analysis can effectively support the identification and selection of optimal mitigation and adaptation strategies. By providing a coherent methodological pathway from indicators to strategies, the framework contributes to strengthening the capacity of decision-makers to address complex multi-risk challenges and to promote more resilient and sustainable urban and territorial development pathways.

# 5. Development of life-cycle-oriented multi-objective bridge prioritization strategies at infrastructure scale in a changing climate

## 5.1 Introduction

Bridges within transportation networks are exposed to multiple hazards that may occur either sequentially or simultaneously, rather than as isolated events (Argyroudis et al., 2020). Climate change further intensifies these risks by altering environmental conditions such as precipitation, temperature, and humidity. Increased rainfall leads to more frequent and severe flooding, changes in groundwater conditions, and the activation of landslides, erosion, and soil liquefaction, all of which can exacerbate structural vulnerability (Milić & Marić, 2023). At the same time, temperature and humidity variations contribute to material degradation, including corrosion in reinforced concrete and cracking due to thermal stresses (Nasr et al., 2020; Milić & Marić, 2023; Nava et al., 2023).

As bridges age, deterioration processes such as corrosion significantly increase their susceptibility to damage, especially when combined with external hazards like earthquakes and floods. These interacting factors highlight the need for integrated approaches to risk assessment and management. The concept of resilience is therefore essential, referring to the ability of infrastructure systems to withstand hazards and recover functionality efficiently (Bruneau et al., 2003).

Effective resilience management requires life-cycle assessment, condition monitoring, and optimized allocation of limited resources for maintenance and rehabilitation. Traditional assessments typically address hazards individually and focus on direct physical damage. Such approaches do not capture cumulative damage effects, network-level consequences, or indirect socio-economic losses. A holistic evaluation therefore requires metrics capable of representing system performance under compound and evolving risk conditions. Recent research has proposed probabilistic and resilience-based frameworks to prioritize interventions, accounting for aging, damage accumulation and single hazard (Capacci et al., 2022, Jafari et al., 2023; Jafari et al., 2024). This study extends such results to multi-hazard scenarios, integrating seismic events, flooding, and environmental deterioration processes influenced by climate change. The proposed approach, presented in (Jafari and Biondini, 2025), integrates structural vulnerability, network functionality, recovery processes, and socio-economic impacts within a unified decision framework. The proposed methodology is intended to support the prioritization of preventive and restorative interventions over the life cycle of infrastructure systems exposed to concurrent hazards, deterioration, and climate change effects.

## 5.2 Methodology

### 5.2.1 Multi-Hazard Vulnerability under Climate Change and Network Damage Representation

Structural vulnerability of bridges is characterized using probabilistic fragility models that relate hazard intensity and structural condition to the likelihood of reaching different damage states. As described above, climate change has become a major concern in infrastructure management, as it can increase the intensity and frequency of extreme events, particularly flooding, thereby elevating hazards such as scour around bridge foundations. Failure to account for these changes may lead to underestimation of structural vulnerability. Climate change also accelerates material deterioration through rising temperatures and elevated $CO_2$ concentrations, which increase carbonation depth and chloride penetration in reinforced concrete. The combined effects of intensified hazards and accelerated aging significantly heighten structural vulnerability and worsen the consequences of extreme events. Therefore, over their service life, each bridge of a network is exposed to a combination of:

- Natural hazards (e.g., earthquakes, floods)

- Sequential events (e.g., mainshock–aftershock sequences)
- Environmental degradation and aging
- Climate-driven changes in hazard severity and deterioration rates

Accordingly, in a multi-hazard context, fragility models have also to account for factors such as aging, environmental deterioration, prior damage, and retrofit interventions, which influence structural capacity and performance under hazardous events. In this work, these effects are incorporated into the bridge network fragility representation through modification factors applied to existing as-built fragility curves, adjusting the median intensity measures to reflect changes in structural capacity:

$$P\left[S_b \geq s_b \mid \hat{s}_b, r_b, r_{b,Sc}, i_b, t_b, Sc_b\right] = \Phi\left[\frac{\ln(i_b) - \ln(MF_a(s_b, t_b, T, RH) \cdot MF_{Sc}(s_b, Sc_b) \cdot MF(s_b, \hat{s}_b, r_b) \cdot MF_{Sc,r}(s_b, r_{b,Sc}, Sc_b) \cdot i_{b,m}(s_b))}{\zeta_{s,b}(s_b)}\right], \quad (1)$$

$$s_b > \hat{s}_b$$

Here, Sb represents the damage state of the b-th bridge in the network; ŝb represents the pre-existing damage state of bridge; rb denotes the seismic retrofit method; rb,Sc is retrofit method enhancing bridge strength against flood-induced scour; ib signifies the seismic intensity at the b-th bridge site; tb stands for bridge age; Scb is scour depth at the b-th bridge site; MFa (sb, tb, T, RH) represents the modification factor for median values of fragility curves for damage state sb, considering the bridge age tb at the occurrence time of hazards integrating the consequences of anticipated shifts in temperature T and relative humidity RH due to climate change, which affect the corrosion process; MFSc (sb, Scb) accounts for the effect of scour depth on bridge vulnerability; MF (sb, ŝb, rb) incorporates the influence of seismic retrofit and pre-existing damage; MFSc,r (sb, rb,Sc, Scb) presents the effect of flood retrofitting measures; ib,m (sb) represents the median seismic intensity measure leading to the exceedance of a given damage state sb; ζs,b(sb) is the standard deviation of the natural logarithm of the seismic intensity measure leading to the exceedance of a given damage state sb.

Network-level conditions are obtained by combining the damage states of individual bridges. Expected damage levels are derived from the probabilistic distribution of states and discretized into representative categories. The resulting network damage description reflects spatial variability and heterogeneous performance across the system, enabling assessment of functionality under partial disruption.

### 5.2.2 Resilience Metric Based on Network Functionality

Resilience is quantified as the ability of the network to maintain and recover functionality over time following disruptive events. It is defined by four key properties: robustness (the ability to withstand and maintain service), rapidity (the speed of recovery), redundancy (the availability of alternative systems), and resourcefulness (the ability to mobilize necessary resources for response and recovery). Resilience is measured as the normalized integral of the functionality trajectory from the event occurrence time $t_0$ to a specified horizon $t_h$:

$$R = \frac{1}{t_h - t_0} \sum_{i=1}^{N_t} Q_i \cdot \Delta t \quad (2)$$

Where $t_i$ represents the time corresponding to step $i$; $\Delta t$ is the duration of each equal time interval; $N_t$ is the total number of time steps; and $Q_i$ denotes network functionality at time step $i$.

Network functionality is assessed using a congestion-based traffic performance metric that reflects operational consequences of bridge damage. The metric accounts for:

- Increased travel times
- Additional travel distances due to detours
- Reduced traffic capacity

- Redistribution of flows across alternative routes

A normalized performance index derived from these quantities provides the functionality measure. This approach directly links bridge structural damage to transportation service degradation experienced by users.

### 5.2.3 Recovery modeling

Post-event recovery is represented as a staged process in which bridges progressively transition to lower damage states over time. Restoration durations depend on damage severity and available resources.

As repairs proceed, traffic capacity is gradually restored, producing a time-dependent functionality profile. Integrating this profile yields the resilience metric, capturing both the magnitude of performance loss and the speed of recovery.

### 5.2.4 Socio-Economic Impact Indicators

Infrastructure disruption affects not only structural performance but also users and economic activity. To reflect these impacts, both direct intervention costs and indirect user costs are evaluated.

Direct costs include expenditures associated with retrofit ($C_{Ret}$) and restoration activities ($C_{Res}$):

$$C_{direct} = C_{Res} + C_{Ret} = \sum_{b=1}^{N_b} c_0 \cdot T_b + \sum_{b=1}^{N_b} \left[ c_b(r_b) + c_b(r_{b,Sc}) \right] \quad (3)$$

where $c_0$ represents the unit-time intervention cost for restoration; $T_b$ denotes the duration of restoration for bridge $b$; $c_b(r_b)$ corresponds to the cost associated with the selected seismic retrofit type $r_b$ and $c_b(r_{b,Sc})$ represents the cost of flood retrofit.

These costs represent the financial requirements for implementing intervention strategies. Indirect losses arise from transportation disruptions and include:

- Vehicle operation costs due to detours and congestion ($C_{run}$)
- Personnel and goods delay costs ($C_{TL}$)
- Casualty costs ($C_{SL}$)

Vehicle operation costs are estimated from changes in total travel time (TTT) and distance (TTD):

$$C_{run}(s) = [TTT(s) - TTT(1)] \cdot [TTD(s) - TTD(1)] \cdot [c_{run,car}(1 - \rho_{truck}) + c_{run,truck}\rho_{truck}] \quad (4)$$

Where $TTT(s)$ and $TTD(s)$ represent the total travel time and total travel distance, respectively, of traffic flows in the bridge network under damage condition $s$. $TTT(1)$ and $TTD(1)$ correspond to the total travel time and distance in the undamaged network. The factors $c_{run,car}$ and $c_{run,truck}$ refer to the average running costs (\$/km) for cars and trucks, respectively. $\rho_{truck}$ represents the proportion of trucks in the traffic flow; this ratio enables trucks to be expressed in car-equivalent terms for consistent analysis. As previously mentioned, to evaluate the bridge network's functionality, a combined traffic assignment and trip distribution approach is applied. In this method, all vehicles in the traffic flow are uniformly measured in car-equivalents per hour (cars/h).

Costs associated with storing personnel and goods due to detours represent the monetary value of time lost by passengers and cargo as a result of delays when traveling through detour routes and affected links:

$$C_{TL}(s) = [TTT(s) - TTT(1)] \cdot [c_{AW} \cdot O_{car}(1 - \rho_{truck}) + (c_{ATC} \cdot O_{truck} + c_{good})\rho_{truck}] \quad (5)$$

Where $c_{AW}$ denotes the average wage per hour (\$/h), $c_{ATC}$ represents the average total compensation per hour (\$/h), and $c_{goods}$ captures the time value of cargo (\$/h), effectively signifying the price of goods transportation; meanwhile, $O_{car}$ and $O_{truck}$ indicate the average vehicle occupancies for cars and trucks, respectively.

Casualty-related costs are based on the number of fatalities and injuries resulting from bridge damage:

$$C_{SL}(s) = \sum_{b=1}^{N_b} FT(s_b) \cdot ICAF \quad (6)$$

Where $FT(s_b)$ represents the average number of fatalities linked to a particular bridge damage state, derived from statistical analysis of observed casualties following a hazard, and $ICAF$ refers to the implied cost of averting a fatality in bridge engineering.

Total indirect impacts are obtained by aggregating these components over the recovery period:

$$C_{indirect} = \sum_{i=1}^{N_t} [C_{run}(s(t_i)) + C_{TL}(s(t_i)) + C_{SL}(s(t_i))] \quad (7)$$

Where $t_i$ represents the $i$ -th time step out of a total of $N_t$ steps, used to calculate the indirect loss over the specified time horizon; $s(t_i)$ is the bridge network damage condition at $t_i$.

### 5.2.5 Integrated Prioritization Framework

The methodology supports coordinated planning of interventions through a multi-objective optimization framework that considers three performance dimensions:

- Network resilience (system functionality over time)
- Direct rehabilitation costs (agency perspective)
- Indirect user costs (societal perspective)

Decision variables include pre-event retrofit strategies and the timing of post-event restoration activities, subject to resource constraints. The framework generates sets of optimal solutions representing trade-offs among objectives, enabling informed selection of intervention strategies.

The framework is consistent with the four fundamental properties of resilience: robustness is addressed through pre-event retrofitting that enhances structural capacity; rapidity is achieved by optimizing post-event restoration timing to accelerate recovery; resourcefulness is reflected through constraints related to available repair resources and budget limitations; and redundancy, while not modelled directly, is captured through the evaluation of network performance under various damage scenarios. Specifically, if a bridge is damaged but traffic can still reroute through alternate paths using less-damaged or undamaged bridges and the use of detours, the network exhibits redundancy. This behaviour is reflected in performance metrics such as increased travel time, longer travel distances, and detour reliance, allowing the framework to assess redundancy through its impact on overall functionality.

## 5.3 Illustrative application

The approach has been applied to a hypothetical bridge network composed of six bridges (Figure 1) with different structural characteristics. The network represents a simplified transportation system in which bridges differ in structural configuration and age, while alternative routes are assumed to be available in case of damage. It is intended to reflect conditions typical of regions exposed to multiple hazards, particularly earthquakes and floods, where infrastructure systems may experience both seismic events and flood-induced scour at river crossings. The considered scenario includes:

- A seismic mainshock followed by multiple aftershocks
- Flood-induced scour affecting selected bridges
- Bridges with different ages and deterioration levels
- Availability of detour routes

Hazard intensities (Figure 2) are considered through representative seismic and flood scenarios under climate change, while factors such as structural type, bridge aging, and the presence of detour routes are incorporated to approximate realistic operating conditions of bridge networks exposed to multi-hazard

environments and evolving climate-related risks. Various retrofit and restoration strategies are evaluated to identify intervention plans that enhance resilience while controlling economic impacts.

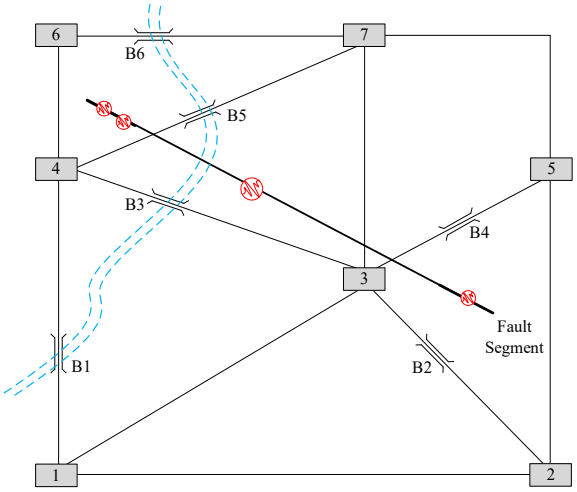


Figure 1: Bridge Network Layout

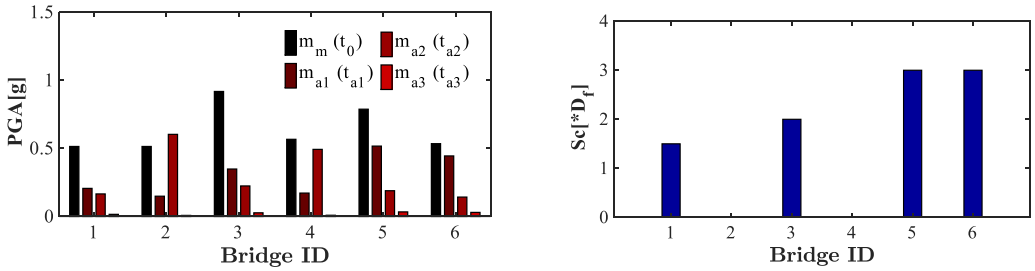


Figure 2: Hazard intensities: (a) Seismic demands at bridge sites associated with mainshock and aftershocks; (b) Scour depth considering the effect of climate change (multiple of foundation depth $D_f$)

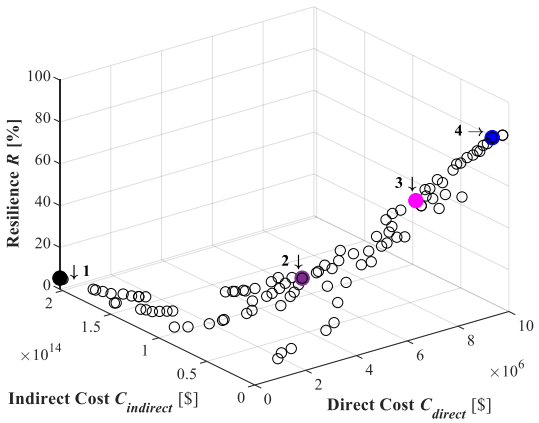


Figure 3: Pareto fronts illustrating the full set of optimal solutions, with four solutions highlighted for detailed representation

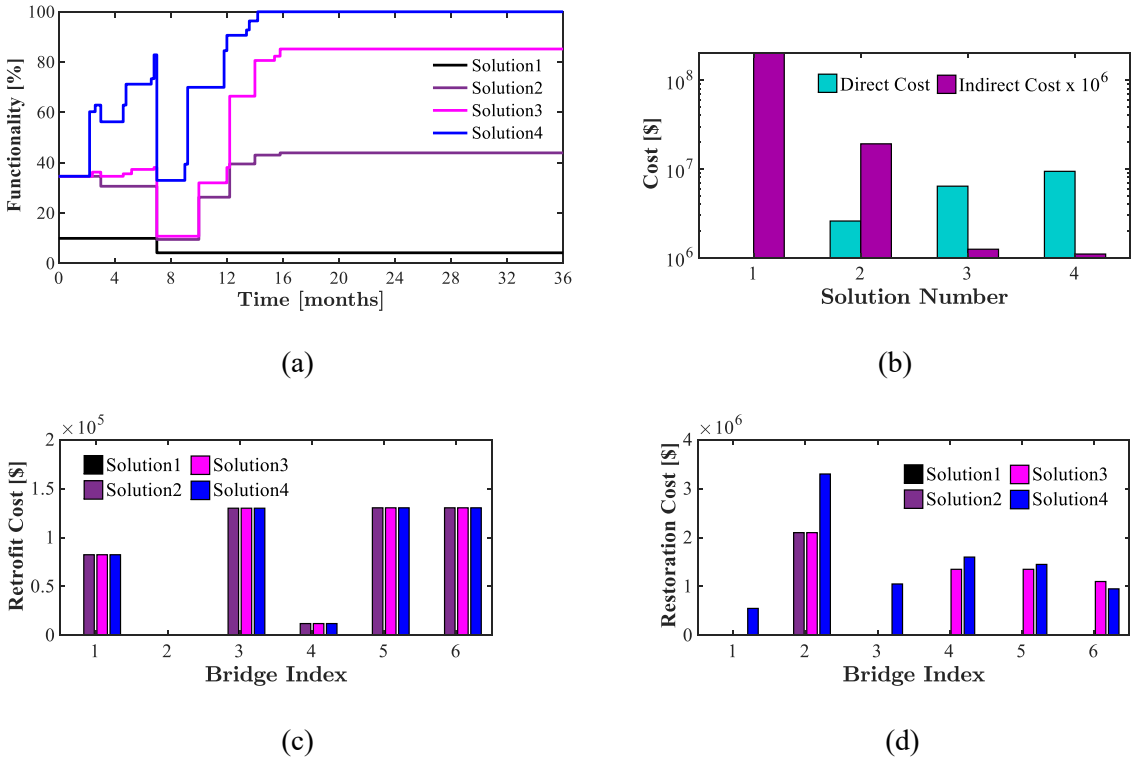


Figure 4: Representations for selected Pareto front solutions: (a) Network functionality with recovery profiles of the selected solution; (b) Direct and indirect costs; (c) Retrofit costs and (d) Restoration costs

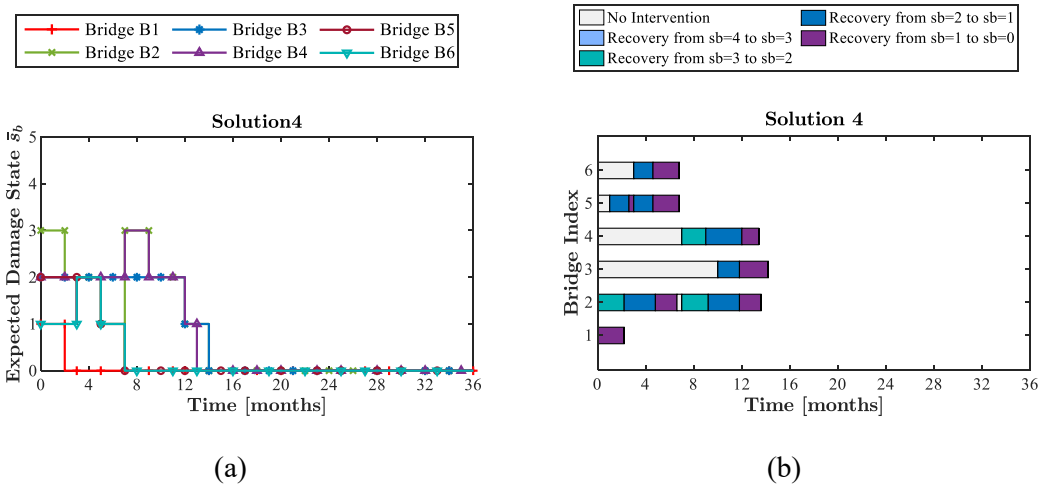


Figure 5: (a) Expected damage states profile for solution #4 selected from Pareto-Front; (b) Repair schedules associated with solution #4 selected from Pareto-Front

The Pareto fronts (Figure 3) obtained from the framework, are effective in assisting stakeholders in selecting strategies aligned with budgetary constraints, indirect loss targets, and available resources, including labour and equipment. In fact, each optimal solution in the front includes detailed time profiles illustrating network functionality, bridge damage progression, and associated direct and indirect costs (Figure 8), accompanied by Gantt charts as practical graphical decision-support tools to enable prompt and informed actions (Figure 9)

## 5.4 Conclusions

This study presents a life-cycle-oriented, resilience-based multi-objective framework for the prioritization of interventions in aging bridge networks exposed to multiple hazards under changing climate conditions. By integrating seismic events, flood-induced scour, and time-dependent deterioration processes, the proposed methodology provides a comprehensive representation of infrastructure performance under compound and evolving risk scenarios.

The results highlight the critical role of accounting for both hazard interactions and climate-driven effects, which significantly influence structural vulnerability and network functionality. The incorporation of probabilistic fragility models, coupled with network-level performance metrics, enables a realistic assessment of damage propagation and its impact on transportation services.

The proposed multi-objective optimization framework allows decision-makers to identify optimal trade-offs between resilience enhancement, direct intervention costs, and indirect socio-economic impacts. By jointly considering pre-event retrofitting and post-event recovery strategies under resource constraints, the methodology supports informed and cost-effective planning of infrastructure management actions.

The application to a representative bridge network demonstrates the effectiveness of the approach in capturing the benefits of proactive adaptation and strategic rehabilitation. In particular, the results show that integrating climate change effects and deterioration processes into the decision framework leads to more robust and future-proof intervention strategies.

Overall, the study contributes to advancing multi-hazard infrastructure risk assessment by providing a scalable and physically consistent tool for resilience-based decision-making. The proposed framework can support infrastructure managers and policymakers in improving the long-term performance and sustainability of transportation networks in increasingly complex hazard environments.

# 6. Development of a multi-objective decisions making tool to optimized the budget distribution for proactive strengthening in seismic regions and reactive repairs post-earthquake

## 6.1 Introduction

The large number of casualties and injuries and the extensive damage to the building stock and production activities generated by seismic events have highlighted the need to plan and implement interventions aimed at reducing the seismic vulnerability of the existing building stock.

Earthquakes repeatedly cause severe human and economic losses, especially in historic urban areas with vulnerable masonry buildings (Marques et al. 2018; Maio et al. 2020). Although many retrofitting techniques exist (Gkournelos et al. 2021, 2022), limited resources make it impossible to strengthen entire building stocks, making budget optimisation essential (Nuzzo et al. 2021; Vona et al. 2017).

The literature provides various procedures for prioritising seismic interventions, often combining visual screening, simplified vulnerability assessments, probabilistic approaches and multi-criteria decision-making. These methods have been applied to buildings, schools, bridges and hospitals, offering useful tools for ranking interventions. However, most studies rely on deterministic assumptions, which are unsuitable in seismic contexts characterised by strong uncertainty. Multi-criteria analyses have also compared alternative retrofit strategies, showing that no single solution is optimal across structural, economic and functional criteria. Yet, these works do not address the joint optimisation of pre-event strengthening and post-event repair, nor the allocation of resources across uncertain scenarios. Only a few contributions consider stochastic budget allocation, mostly outside the seismic field. Thus, probabilistic formulations for seismic mitigation remain largely unexplored.

This study fills this gap by proposing a two-stage stochastic model to allocate a limited budget between Proactive Strengthening (PS) and Reactive Repair (RR), aiming to minimise expected evacuees after earthquakes. First-stage variables define strengthening actions; second-stage variables determine repair strategies under alternative damage scenarios. The model uses an innovative exposure–vulnerability assessment based on the CARTIS procedure under development in Italy (Zuccaro et al. 2015; Cacace et al. 2018; Dolce et al. 2021), and incorporates vulnerability levels, intervention costs and expected vulnerability reductions (MIT 2018; FEMA 1994; DPCI 2021; Di Ludovico et al. 2022). The stochastic solution is compared with a purely reactive strategy and applied to a real case study in Sicily. The novelty lies in allowing multiple strengthening intensities per building and optimally splitting the budget between PS and RR, with post-earthquake losses depending on pre-event actions. To the authors' knowledge, no previous study has formulated a stochastic optimisation model to minimise earthquake-induced evacuees.

## 6.2 Method and definition of input variables

This section presents a structured methodology for evaluating seismic vulnerability, defining effective risk-reduction strategies, and estimating associated intervention costs for residential buildings in seismic areas. The analysis requires four key inputs: (i) building exposure data, (ii) vulnerability assessment, (iii) intervention types and their effectiveness in reducing vulnerability, and (iv) intervention costs. The approach combines survey information, engineering assessment methods, and cost models to provide a cohesive framework for analysing the economic impacts of seismic events. The section is organised into subsections covering intervention types, cost analysis, vulnerability assessment, and damage scenario development.

### 6.2.1 Intervention types

Extensive research has examined strengthening techniques for masonry and reinforced concrete buildings due to their high seismic vulnerability. The Italian Code (MIT 2018) defines three intervention levels used in

this study: seismic retrofitting, which upgrades structural capacity to meet safety standards for new buildings ($\varsigma_E \geq 0.8–1$); seismic improvement, which increases safety without reaching retrofit performance levels; and local strengthening, which targets specific vulnerable elements without altering the overall structural behaviour, though it may still enhance global performance.

### 6.2.2 Cost analysis

Cost estimation for seismic retrofitting has traditionally relied on expert judgment and regression models (Jafarzadeh et al. 2014a), with more recent developments using neural networks, Bayesian regression, and machine-learning approaches (Jafarzadeh et al. 2014b; Nasrazadani et al. 2017; Safaeian Hamzehkolaei & Alizamir 2021). Additional contributions include taxonomies for direct and indirect costs (Fung et al. 2021) and cost models for Italian masonry buildings (Follador et al. 2024).

In this study, intervention costs are derived from FEMA (1994), which provides cost tables for structural strengthening across four seismicity levels. Only the table for very high seismicity is reported here (Table 3b). Costs are referenced as C01–C04, corresponding to low, moderate, high, and very high seismicity. To align FEMA values with recent Italian data, all costs are scaled by a coefficient a = 23.30, obtained by comparing DPCI 2021 retrofit costs with FEMA values; updated costs are therefore $C_{Ui} = C_{0i} \times a$ (i=1,2,3,4)..

Because exposure data follow the CARTIS classification, while costs follow FEMA typologies, EMS98 structural classes (Table 3a) were mapped to FEMA categories (Table 3b). For example, EMS98 types M1 and M3 correspond to FEMA URM, while RC1–RC3 correspond to FEMA C1/C3.

Table 3 - Building typologies: a) EMS98 macroseismic scale (EMS98); b) FEMA (FEMA 1994)

a)

| Typologies | Code | Building Type | Characteristic Values of the Vulnerability Index | | | | |
|---|---|---|---|---|---|---|---|
| | | | $VI_{min}$ | $VI^-$ | $VI^*$ | $VI^+$ | $VI_{max}$ |
| Masonry | M1 | Rubble stone | 0.62 | 0.81 | 0.873 | 0.98 | 1.02 |
| | M2 | Adobe/earth bricks | 0.62 | 0.687 | 0.84 | 0.98 | 1.02 |
| | M3 | Simple stone | 0.46 | 0.65 | 0.74 | 0.83 | 1.02 |
| | M4 | Massive stone | 0.3 | 0.49 | 0.616 | 0.793 | 0.86 |
| | M5 | U Masonry (old bricks) | 0.46 | 0.65 | 0.74 | 0.83 | 1.02 |
| | M6 | U Masonry - r.c. floors | 0.3 | 0.49 | 0.616 | 0.79 | 0.86 |
| | M7 | Reinforced /confined masonry | 0.14 | 0.33 | 0.451 | 0.633 | 0.7 |
| Reinforced concrete | RC1 | Frame in RC (without E.R.D.)* | 0.3 | 0.49 | 0.644 | 0.8 | 1.02 |
| | RC2 | Frame in RC (moderate E.R.D.) * | 0.14 | 0.33 | 0.484 | 0.64 | 0.86 |
| | RC3 | Frame in RC (high E.R.D.) * | −0.02 | 0.17 | 0.324 | 0.48 | 0.7 |
| | RC4 | Shear walls (without E.R.D.) * | 0.3 | 0.367 | 0.544 | 0.67 | 0.86 |
| | RC5 | Shear walls (moderate E.R.D.) * | 0.14 | 0.21 | 0.384 | 0.51 | 0.7 |
| | RC6 | Shear walls (high E.R.D.) * | −0.02 | 0.047 | 0.224 | 0.35 | 0.54 |
| Steel | S | Steel structures | −0.02 | 0.17 | 0.324 | 0.48 | 0.7 |
| Wood | W | Wood structures | 0.14 | 0.207 | 0.447 | 0.64 | 0.86 |

*E.R.D. stands for "Earthquake Resistant Design"

b)

| TYPICAL STRUCTURAL COSTS FOR VERY HIGH SEISMICITY AND LIFE SAFETY ($/sq.ft.) | | | | | | |
|---|---|---|---|---|---|---|
| Building group | Model | FEMA Building types | Area | | | |
| | | | Small | Medium | Large | V-Large |
| 1 | URM | Unreinforced Masonry | 18.22 | 18.04 | 17.14 | 14.43 |
| 2 | W1 | Wood Light Frame | 14.07 | 14.79 | 18.56 | 23.78 |
| | W2 | Wood (Commercial or Industrial) | | | | |
| 3 | PC1 | Precast Concrete Tilt Up Walls | 18.69 | 17.7 | 15.52 | 9.43 |
| | RM1 | Reinforced Masonry with Metal or Wood Diaphragm | | | | |
| 4 | C1 | Concrete Moment Frame | 25.75 | 25.04 | 23.86 | 19.84 |
| | C3 | Concrete Frame with Infill Walls | | | | |
| 5 | S1 | Steel Moment Frame | 25.82 | 25.37 | 24.26 | 18.47 |
| 6 | S2 | Steel Braced Frame | 10.07 | 9.56 | 7.68 | 4.35 |
| | S3 | Steel Light Frame | | | | |
| 7 | S5 | Steel Frame with Infill Walls | 29.47 | 29.28 | 28.05 | 24.65 |
| 8 | C2 | Concrete Shear Wall | 22.67 | 22.06 | 20.83 | 16.95 |
| | PC2 | Precast Concrete Frame with Concrete Shear Walls | | | | |
| | RM2 | Reinforced Masonry with Precast Concrete Diaphragm | | | | |
| | S4 | Steel Frame with Concrete Walls | | | | |

Once the EMS98–FEMA typology mapping was defined, the four FEMA cost levels - corresponding to low, medium, high, and very high seismicity ($a_g$ < 0.05g, 0.15g, 0.25g, 0.35g) - were assigned to each building type. These costs (CU1–CU4) represent seismic retrofitting costs at the respective seismicity levels. By shifting these values across seismicity classes, the same FEMA costs can also be used to represent seismic improvement actions (e.g., CU3 is an improvement cost when applied to a very high seismicity area).

This logic does not apply to local strengthening, since using CU2–CU4 directly would yield unrealistic cost ratios. Based on literature, the typical ratio between local strengthening and full retrofitting is about 0.24, which is adopted here. Table 4 summarises the criteria used to assign retrofit, improvement, and local strengthening costs for each seismicity level.

Table 4 - Updated costs for different intervention levels in different seismicity areas ($C_{Ui}=C_{0i}*a$)

| | Low Seismicity (€/m²) | Medium seismicity (€/m²) | High seismicity (€/m²) | Very high seismicity (€/m²) |
|---|---|---|---|---|
| **Local strengthening** | $0.24*C_{U1}$ | $0.24*C_{U2}$ | $0.24*C_{U3}$ | $0.24*C_{U4}$ |
| **Seismic improvement** | $0.5*C_{U1}$ | $C_{U1}$ | $C_{U2}$ | $C_{U3}$ |
| **Seismic retrofitting** | $C_{U1}$ | $C_{U2}$ | $C_{U3}$ | $C_{U4}$ |

The model also requires repair cost data for five post-earthquake damage levels (D1–D5), derived from the reconstruction of RC and masonry buildings after the 2009 L'Aquila earthquake (Di Ludovico et al. 2022). These direct repair costs are expressed as percentages of the reference unit cost for new construction (1350 €/m²). Damage states follow the EMS98-based classification of Lagomarsino and Giovinazzi (2006), with D0 indicating no damage.

Because post-earthquake losses also include indirect costs**,** especially population assistance expenses (Mannella et al. 2017), the model incorporates both direct repair costs (Table 5) and assistance costs (Table 6), the latter also expressed as a percentage of the reference unit cost. In the following, the term *repair cost* refers to the combined total of these two components.

Table 5 - % $C_r$ as a function of Damage States (DS) (Di Ludovico et al. 2022)

| | 4.664 RC buildings | | | | | 3.833 masonry buildings | | | | |
|---|---|---|---|---|---|---|---|---|---|---|
| **Damage states** | **DS1** | **DS2** | **DS3** | **DS4** | **DS5** | **DS1** | **DS2** | **DS3** | **DS4** | **DS5** |
| **N. of buildings** | 1.835 | 690 | 643 | 194 | 20 | 941 | 276 | 292 | 92 | 81 |
| **%Cr – 16th percentile** | 0% | 6% | 14% | 26% | 44% | 0% | 8% | 16% | 25% | 34% |
| **%Cr – median** | 3% | 14% | 34% | 59% | 81% | 4% | 17% | 33% | 52% | 72% |
| **%Cr – 84th percentile** | 13% | 29% | 64% | 95% | 107% | 17% | 5% | 78% | 96% | 95% |
| **%Cr – mean** | 6% | 19% | 39% | 62% | 78% | 8% | 22% | 41% | 59% | 67% |
| **%C – standard deviation** | 10% | 18% | 26% | 32% | 32% | 10% | 18% | 28% | 33% | 29% |
| **%Cr – CoV** | 64% | 105% | 149% | 195% | 191% | 76% | 116% | 157% | 163% | 235% |

Table 6 - Percentage assistance costs with respect to reference unit costs, % $C_a$, as a function of Damage State (DS) (Di Ludovico et al. 2022)

| | 4.329 RC buildings | | | | | 3.518 masonry buildings | | | | |
|---|---|---|---|---|---|---|---|---|---|---|
| **Damage states** | **DS1** | **DS2** | **DS3** | **DS4** | **DS5** | **DS1** | **DS2** | **DS3** | **DS4** | **DS5** |
| **N. of buildings** | 1.753 | 608 | 536 | 152 | 16 | 869 | 217 | 216 | 64 | 49 |
| **%Ca – 16th percentile** | 0% | 3% | 8% | 11% | 15% | 0% | 4% | 7% | 8% | 9% |
| **%Ca – median** | 0% | 10% | 20% | 25% | 38% | 0% | 11% | 16% | 19% | 18% |
| **%Ca – 84th percentile** | 10% | 25% | 37% | 40% | 47% | 11% | 24% | 36% | 29% | 46% |
| **%Ca – mean** | 4% | 14% | 23% | 27% | 35% | 5% | 14% | 21% | 22% | 23% |
| **%Ca – standard deviation** | 9% | 14% | 16% | 15% | 17% | 10% | 13% | 15% | 17% | 17% |
| **%Ca – CoV** | 206% | 95% | 71% | 55% | 51% | 206% | 93% | 74% | 78% | 75% |

### 6.2.3 Exposure and vulnerability assessment

Exposure data were collected using the CARTIS survey (Zuccaro 2004; Zuccaro et al. 2015; Colajanni et al. 2023), while vulnerability was assessed through the Macroseismic (Lagomarsino & Giovinazzi 2006) and Heuristic (Lagomarsino et al. 2021) methods. The effectiveness of each intervention is quantified by the resulting reduction in the vulnerability index, requiring the definition of a target vulnerability value representative of new constructions.

For RC buildings, the Macroseismic method provides a reference value of V = 0.324, adopted here for retrofitted structures. For masonry buildings, target values are derived from Lagomarsino et al. (2021), which relate vulnerability to construction year and building height (Table 7); in the absence of post-2008 data, estimated values for recent masonry buildings are used. A representative target value of V ≈ 0.30 is selected.

For consistency across construction types, a uniform target vulnerability value of V = 0.3 is adopted for both RC and masonry buildings.

To compute the vulnerability index of buildings post-intervention ($V_f$) from their initial vulnerability indices (Vi) as described earlier, the following formula is employed:

$$V_f = (V_i) + (V_a - V_i) * \alpha = (V_i) + \delta_{i,C} \quad (C=H,M,L) \quad (1)$$

The formula updates each building's vulnerability index by combining its initial value $V_i$, the target value for a new structure ($V_a$=0.3), and the achievable reduction $\delta_{i,C}$. The parameter α reflects the intervention level: 1 (or 0.8 per MIT 2018) for seismic retrofitting, 0.55 for improvement, and 0.20 for local strengthening. This formulation is used to compute post-intervention vulnerability for all construction typologies. The authors note that, for practical applications, α should be locally recalibrated and a more accurate (nonlinear) relationship may be required.

Table 7 - Vulnerability indices representative of the ISTAT masonry sub-types (Lagomarsino et al. 2021)

| ISTAT sub-type | A1 (<1919) | | | A2 (1919-1945) | | | A3 (1946-1961) | | | A4 (1962-1981) | | | A5 (>1981) | | |
|---|---|---|---|---|---|---|---|---|---|---|---|---|---|---|---|
| | L | M | H | L | M | H | L | M | H | L | M | H | L | M | H |
| V | 0.92 | 0.88 | 0.98 | 0.82 | 0.76 | 0.88 | 0.68 | 0.70 | 0.74 | 0.52 | 0.56 | 0.60 | 0.40 | 0.42 | 0.44 |

### 6.2.4 Damage scenarios

Damage scenarios were generated for selected PGA levels using fragility curves: the Heuristic method (Lagomarsino et al. 2021, Colajanni and D'Anna 2023) for masonry buildings and the Macroseismic method (Lagomarsino and Giovinazzi, 2006) for RC buildings. For each PGA and damage state "k", the minimum vulnerability value $V_{min,k}$ required to reach that damage level was identified. Under a deterministic approach, $V_{min,k}$ is obtained from the mean PGA of the fragility curve corresponding to damage level k (Lagomarsino & Giovinazzi 2006; Lagomarsino et al. 2021).

$$PGA_{Dk,Vi,k} = c_1 c_2^{[6,7-3,45Vi+(0,9+2,8Vi)\ atanh(0,36k-1,08)]} \quad \text{for masonry buildings with Vi>0.38} \quad (2\ a)$$

$$PGA_{Dk,Vi,k} = c_1 c_2^{[8.1-6,25Vi+2,3\ atanh(0,36k-1,08)]} \quad \text{for reinforced concrete buildings} \quad (2\ b)$$

By solving Eq. 2 with respect to the value of $V_i$, the value of $V_{min,k}$ can be calculated for each PGA value and damage level. In particular, the values of $V_{min,k}$ are provided for masonry and RC building, respectively, in Table 8.

Table 8 - Minimum values of vulnerability index $V_{min,k}$ for pre-established PGA values for which the k damage level is achieved

| **TR [years]** | 30 | 50 | 72 | 101 | 140 | 201 | 475 | 975 | 2475 | 10000 |
|---|---|---|---|---|---|---|---|---|---|---|
| **Ag [g]** | 0.060 | 0.079 | 0.094 | 0.110 | 0.126 | 0.145 | 0.197 | 0.248 | 0.324 | 0.438 |
| | | | | | **Masonry** | | | | | |
| **D0** | | | | | | | | | | |
| **D1** | 1.112 | 1.007 | 0.941 | 0.882 | 0.830 | 0.777 | 0.661 | 0.573 | 0.472 | 0.357 |
| **D2** | 1.365 | 1.242 | 1.164 | 1.094 | 1.033 | 0.971 | 0.834 | 0.731 | 0.612 | 0.477 |
| **D3** | 1.838 | 1.680 | 1.581 | 1.491 | 1.413 | 1.333 | 1.158 | 1.026 | 0.873 | 0.701 |
| **D4** | 2.679 | 2.461 | 2.322 | 2.198 | 2.090 | 1.978 | 1.734 | 1.551 | 1.339 | 1.099 |
| **D5** | 4.053 | 3.735 | 3.533 | 3.351 | 3.194 | 3.031 | 2.676 | 2.409 | 2.099 | 1.750 |
| | | | | | **Reinforced concrete** | | | | | |
| **D0** | | | | | | | | | | |
| **D1** | 1.009 | 0.922 | 0.867 | 0.817 | 0.775 | 0.730 | 0.633 | 0.561 | 0.476 | 0.381 |
| **D2** | 1.111 | 1.024 | 0.970 | 0.920 | 0.877 | 0.833 | 0.736 | 0.663 | 0.579 | 0.484 |
| **D3** | 1.238 | 1.152 | 1.097 | 1.047 | 1.004 | 0.960 | 0.863 | 0.790 | 0.706 | 0.611 |
| **D4** | 1.366 | 1.279 | 1.224 | 1.174 | 1.131 | 1.087 | 0.990 | 0.918 | 0.833 | 0.738 |
| **D5** | 1.468 | 1.381 | 1.326 | 1.277 | 1.234 | 1.190 | 1.093 | 1.020 | 0.936 | 0.841 |

In order to derive the number of evacuees for each damage level suffered by a building, an average number of square meters of Habitable Surfaces per Inhabitant HSpI ($m^2$), and a percentage of evacuee by level of damage $p_k$ (k=1-5) must be defined for each type of construction.

## 6.3 Model for cost-benefit analysis

This chapter introduces a deterministic procedure for assessing the economic efficiency of resource allocation between proactive strengthening and reactive repair, with the goal of minimizing evacuees. The analysis considers building vulnerability, intervention costs, seismic intensity, habitable surface per inhabitant (HSpI), and the percentage of evacuees per damage state. Two scenarios are examined: one assuming constant evacuee rates across damage levels and another using damage-dependent rates.

Under deterministic assumptions, intervention priorities can be identified to optimise budget allocation for reducing total evacuees. Table 8 provides the vulnerability thresholds corresponding to each damage level for fixed PGA values, for both masonry and RC buildings. Applying Eq. 1, the final vulnerability index after an intervention is obtained, enabling the expected damage level to be determined using Table 8.

To quantify the cost required to reduce the number of evacuees by one unit ($C_{R1E}$), the intervention cost for the seismicity level of interest, $\beta \cdot C_{Ui}$ (€/m²) (with $\beta$ = 0.24, 0.5, or 1 and $C_{Ui}$ from Table 4), is multiplied by HSpI and divided by the change in evacuation rate between the initial and final damage states, $p_{ki} - p_{kf}$ This deterministic prioritization procedure is applied to the case study in Section 6.5.

## 6.4 A two-stage stochastic model for budget allocation

This section outlines the two-stage stochastic model used to optimise the allocation of resources between proactive strengthening and reactive repair, with the goal of minimizing evacuees under multiple damage scenarios and a fixed budget. In the first stage (pre-earthquake), buildings and intervention types are selected within the available budget, reducing initial vulnerability. In the second stage (post-earthquake), repair actions are chosen for each scenario based on the remaining budget and the damages resulting from first-stage decisions. Proactive and reactive strategies represent opposite allocation philosophies, with fully proactive and fully reactive approaches as limiting cases.

Damage severity depends on the strengthening applied, and unrepaired buildings cause evacuation of a percentage $p_k$ of occupants. Each building i in the set I is defined by construction type, surface $s_i$, inhabitants $w_i$, initial vulnerability $V_i$, strengthening costs ($b_1$, $b_2$, $b_3$) and corresponding vulnerability reductions ($\delta_{i1}$, $\delta_{i2}$, $\delta_{i3}$). Damage states range from D1 to D5 (set K), with $c_{ik}$ representing the repair cost at damage level k. The total budget is B.

Earthquake scenarios S are defined through different PGA values. For each scenario s and each building, the vulnerability threshold aiks triggering damage level k is obtained by perturbing the reference value $V_{min,k}$ from Table 8 within the range $[V_{min,k} - 0.05, V_{min,k} + 0.05]$, accounting for variability in structural response and the fact that earthquakes with the same PGA may produce different damages.

Stochastic variables include building vulnerability, the PGA defining each scenario, and the PGA thresholds associated with each damage level. The objective is to minimize the expected number of evacuees, i.e. occupants of buildings whose damages cannot be repaired within the available budget.

The decision variables involved in the model are the following:

- $X_{ij}$: binary variables assuming value 1 if strengthening action of type j is applied to building i, and 0 otherwise;
- $Y_{is}$: binary variables assuming value 1 if building i has been repaired in scenario s, and 0 otherwise;
- $D_{iks}$: binary variables assuming value 1 if building i has suffered damage of level k in scenario s, and 0 otherwise, i.e. in the scenario s, $\sum_{k=1}^{5} D_{iks} = 0$ if the building is undamaged, $\sum_{k=1}^{5} D_{iks} = 1$ if it has suffered any level of damage;

- $Z_{iks}$: binary variables representing the residual damage, assuming value 1 if building i has suffered the damage of level k in scenario s and has not been repaired, and 0 otherwise. It has a unit value if the building is damaged and it has not undergone repair intervention;
- $C_{is}$: variables indicating the cost paid to repair building i in scenario s.

The two-stage mathematical model was formulated as follows:

$$\min \sum_i \sum_s \sum_k p_k \, w_i \, Z_{iks} \tag{3}$$

s.t.

$$\sum_{j=1}^{3} X_{ij} \leq 1 \qquad \forall i \in I \tag{4}$$

$$\sum_i \sum_j c_{ij} \, X_{ij} + \sum_i C_{is} \leq B \qquad \forall s \in S \tag{5}$$

$$Y_{is} + \sum_k Z_{iks} = \sum_k D_{iks} \qquad \forall s \in S \;\; \forall i \in I \tag{6}$$

$$Z_{iks} \leq D_{iks} \qquad \forall s \in S \;\; \forall i \in I \;\; \forall k \in K \tag{7}$$

$$D_{iks} \geq (v_i - \sum_j \delta_{ij} X_{ij}) - a_{iks} - \sum_{l \epsilon \{k+1..Kmax\}} D_{ils} \qquad \forall s \in S \;\; \forall i \in I \;\; \forall k \in K \tag{8}$$

$$\sum_k D_{iks} \leq 1 \qquad \forall s \in S \;\; \forall i \in I \tag{9}$$

$$C_{is} \geq \sum_k c_{ik} D_{iks} - B(1 - Y_{is}) \qquad \forall s \in S \;\; \forall i \in I \tag{10}$$

$$C_{is} \geq 0 \qquad \forall s \in S \;\; \forall i \in I \tag{11}$$

The objective function in Eq. (3) minimizes the expected number of evacuees. Constraints (4) allow each building to receive only one strengthening action, while constraints (5) ensure that the total cost of strengthening and repair does not exceed the budget B. Constraints (6) link damage to either a repair action or, if unrepaired, to the corresponding evacuation rate. Constraints (7) prevent residual damage from exceeding actual damage.

Constraints (8) assign the appropriate damage level by comparing the post-strengthening vulnerability with the scenario-dependent thresholds $a_{iks}$ from Table 6, ensuring consistency with higher-level damages. Constraints (9) guarantee that only one damage level is selected. Constraints (10) compute scenario repair costs: if a building is repaired ($Y_{is} = 1$), the cost matches the associated damage level; if not repaired ($Y_{is} = 0$), the optimization sets $C_{is} = 0$ to satisfy Eq. (3) and Eq. (5). Finally, constraints (11) impose non-negativity of repair costs.

## 6.5 Case study

Focusing on the municipality of Patti, Sicily, this chapter applies the proposed stochastic model to a real-world context. It describes the region's building typologies, vulnerability indices, and simulated damage scenarios to validate the model's effectiveness.

### 6.5.1 Cost benefit analysis

This section illustrates, for a single example scenario, the economic efficiency of allocating resources for seismic interventions using the procedure described in Section 3. The case study is analysed assuming an

earthquake scenario with PGA=0.248g. Strengthening and repair costs for the different intervention levels, previously defined in Section 6.2, are reported for clarity in Table 9.

Table 9 - Strengthening and repair costs for masonry and RC constructions

| STRENGTHENING COSTS (€/m²) | | | REPAIR COSTS (€/m²) | | | | |
|---|---|---|---|---|---|---|---|
| Masonry | Seismic retrofitting | 425.00 | D1 | D2 | D3 | D4 | D5 |
| | Seismic improvement | 320.00 | 176.00 | 486.00 | 837.00 | 1094.00 | 1215.00 |
| | Local strengthening | 102.00 | | | | | |
| Reinforced concrete | Seismic retrofitting | 600.00 | D1 | D2 | D3 | D4 | D5 |
| | Seismic improvement | 453.00 | 135.00 | 446.00 | 837.00 | 1202.00 | 1526.00 |
| | Local strengthening | 144.00 | | | | | |

Using the costs in Table 9 and HSpI = 35 m², two prioritization tables (Table 10 and Table 11) were developed for masonry and RC buildings. Table 10 refers to the Constant Percentage of Evacuees (CPE) case ($p_k$ = 100% for all damage levels), while Table 11 refers to the Variable Percentage of Evacuees (VPE) case ($p_5=p_4=_{p3}$=100%, $p_2$=50%, $p_1$=10%, $p_0$ =0), adopting the values of Di Ludovico et al. (2023). Masonry interventions are highlighted in orange and RC interventions in grey.

The first column reports the intervention priority, the second the strengthening or repair costs (from Table 9), and the third the cost per evacuee reduction. Under CPE, this latter value equals the intervention cost per m² multiplied by HSpI, since $100/(p_k - p_0) = 1$. Each cost corresponds to a given intervention type (fourth column), according to Table 9, and each intervention is applied to buildings whose vulnerability is compared with the thresholds $V_{min,k}$ in Table 8.

Under CPE, the objective is to eliminate evacuees, meaning only actions that can move buildings from any damage level to D0 are considered; partial reductions require additional repair. Accordingly, the first-ranked intervention in Table 10 is local strengthening of masonry buildings, enabling transition from D1 to D0 at the lowest cost.

Table 11 follows the same methodology but reflects the VPE assumptions, where evacuees vary with damage severity. In this case, reducing buildings from higher to lower damage levels—even without reaching D0—becomes convenient. Thus, interventions not favourable under CPE become beneficial, and all intervention types may be advantageous depending on the cost/evacuee ratio. As a result, the prioritization in Table 11 does not necessarily follow increasing intervention cost, but rather increasing efficiency in evacuee reduction.

The deterministic prioritization presented here will be compared with the outcomes of the two-stage stochastic model, which incorporates uncertainties such as variable PGA levels and differing damage outcomes for earthquakes with the same PGA. This is achieved through scenario- and building-specific perturbations of $V_{min,k}$ within $[V_{min,k} - 0.05, V_{min,k} + 0.05]$, as described earlier.

Table 10 - Prioritization of interventions on masonry and RC constructions, in the case of constant percentage of evacuees (CPE) ($p_k$ = 100%) for all damage levels (k=1-5)

| CPE | | | |
|---|---|---|---|
| Priority | Cost (euro/m²) | Cost/evacuee* (euro) | Action |
| I | 102.00 | 3566.00 | Local strengthening of masonry buildings to move from D1 to D0 damage |
| II | 135.00 | 4725.00 | Repair of RC buildings form D1 to D0 damage |
| III | 176.00 | 6143.00 | Repair of masonry buildings from D1 to D0 damage |
| IV | 320.00 | 11206.00 | Seismic improvement of masonry buildings to move from D1 to D0 damage |
| V | 425.00 | 14859.00 | Seismic retrofitting of masonry buildings to move from D1 to D0 damage |
| VI | 445.00 | 15575.00 | Repair of RC buildings form D2 to D0 damage |
| VII | 452.00 | 15820.00 | Seismic improvement of RC buildings to move from D1 to D0 damage |
| VIII | 486.00 | 17010.00 | Repair of masonry buildings form D2 to D0 damage |
| IX | 600.00 | 21000.00 | Seismic retrofitting of RC buildings to move from D1 to D0 damage |
| X | 837.00 | 29295.00 | Repair of RC buildings form D3 to D0 damage |
| XI | 1202.00 | 42053.00 | Repair of RC buildings form D4 to D0 damage |

*Cost to reduce the total number of residual evacuees of one unit $C_{R1E}$

Table 11 - Prioritization of interventions on masonry and RC constructions, in the case of variable percentage of evacuees (VPE) for different damage levels ($p_5$=$p_4$=$p_3$=100%, $p_2$=50%, $p_1$=10%)

| VPE | | | |
|---|---|---|---|
| **Priority** | **Cost (euro/m²)** | **Cost/evacuee* (euro)** | **Action** |
| I | 102.00 | 7132.00 | Local strengthening of masonry buildings to move from D3 to D2 damage. |
| II | 102.00 | 8916.00 | Local strengthening of masonry buildings to move from D2 to D1 damage. |
| III | 144.00 | 10080.00 | Local strengthening of RC buildings to move from D3 to D2 damage. |
| IV | 144.00 | 10080.00 | Local strengthening of RC buildings to move from D4 to D2 damage |
| V | 144.00 | 12600.00 | Local strengthening of RC buildings to move from D2 to D1 damage. |
| VI | 320.00 | 28014.00 | Seismic improvement of masonry buildings to move from D2 to D1 damage |
| VII | 837.00 | 29295.00 | Repair of RC buildings form D3 to D0 damage |
| VIII | 445.00 | 31150.00 | Repair of RC buildings form D2 to D0 damage |
| IX | 486.00 | 34020.00 | Repair of masonry buildings form D2 to D0 damage |
| X | 102.00 | 35662.00 | Local strengthening of masonry buildings to move from D1 to D0 damage |
| XI | 452.00 | 39550.00 | Seismic improvement of RC buildings to move from D2 to D1 damage |
| XII | 1202.00 | 42053.00 | Repair of RC buildings form D4 to D0 damage |
| XIII | 135.00 | 47250.00 | Repair of RC buildings form D1 to D0 damage |
| XIV | 176.00 | 61425.00 | Repair of masonry buildings from D1 to D0 damage |
| XV | 320.00 | 112056.00 | Seismic improvement of masonry buildings to move from D1 to D0 damage |
| XVI | 425.00 | 148590.00 | Seismic retrofitting of masonry buildings to move from D1 to D0 damage |
| XVII | 452.00 | 158200 | Seismic improvement of RC buildings to move from D1 to D0 damage |
| XVIII | 600.00 | 210000 | Seismic retrofitting of RC buildings to move from D1 to D0 damage |

*Cost to reduce the total number of residual evacuees of one unit $C_{R1E}$

### 6.5.2 Optimal budget allocation by stochastic analysis

The stochastic model was applied to the municipality of Patti (Sicily, Italy), which covers about 50.08 km² and includes approximately 3,787 buildings with 13,347 residents. For seismic vulnerability assessment using the CARTIS procedure (Zuccaro 2004; Zuccaro et al. 2015; Colajanni et al. 2023), the area was divided into ten compartments, each containing specific masonry and/or RC typologies. Table 12 reports the compartment distribution, typologies, number of buildings per typology, the initial vulnerability index $V_i$*, the mean sum of modifiers $\Delta V_i$, and the total vulnerability $V_i=V_i^*+\Delta V_{i,m}$, defined according to Lagomarsino and Giovinazzi (2006).

To reduce computational demand, buildings were aggregated into 100 clusters, proportionally distributed across compartments according to typology frequencies. Each cluster groups buildings of the same typological class, with an average size of about 3,787/100 units, adjusted to match actual typology distributions. Clustering also reflects decision-making constraints, as interventions are applied to groups of buildings with predefined characteristics rather than to individual buildings.

The analysis considers ten post-earthquake scenarios, each associated with a randomly generated PGA value assumed uniform across the municipality. PGA is modelled as a random variable following the exceedance probability $P_{vr}(PGA>a_g)=1-\exp(-V_n/T_R)$, where $V_n$ is the nominal life of buildings and $T_R$ the return period defined by the Italian code (MIT 2018). The resulting PGA values for scenarios S1–S10 are: $a_g$=0.248 ($T_R$ = 975) for S1 and S9; $a_g$=0.126 ($T_R$ = 140) for S2; $a_g$=0.324 ($T_R$ = 2475) for S3–S5; $a_g$=0.145 ($T_R$ = 201) for S6 and S10; and $a_g$=0.197 ($T_R$ = 475) for S7 and S8.

The initial vulnerability of each building was modelled as a Gaussian variable, using the mean values in Table 12 and a standard deviation equal to one-third of the range ensuring a 99% probability within the EMS98 limits [$V_{Imin}$,$V_{Imax}$]. Strengthening costs were derived from FEMA values updated with DPCI 2021, and the total cost for building "i" was obtained by multiplying the unit cost by its (randomly distributed) surface area and number of floors, both sampled uniformly from CARTIS typology ranges. Vulnerability reductions were computed through Eq. (1). The number of inhabitants was linked to building surface and modelled as a Gaussian variable with mean HSpI = 35 m² per person and standard deviation 1.67 m².

The optimization model was solved with the Xpress 8.13 solver on a machine with an 11th Gen Intel Core i7-1185G7 and 32 GB RAM. A time limit of 1 hour was imposed for each scenario, and if optimality was not reached, the best available solution was adopted.

Table 12 - Vulnerability indices and percentages of typologies

| Compartment | Tot. Buildings | Typology | N. Buildings | % in compartment | TIP EMS98 | $V_i$* | $\Delta V_{i,m}$ | $V_i$ |
|---|---|---|---|---|---|---|---|---|
| C01 | 854 | MUR 1 | 512 | 60 | M1 | 0.893 | 0.067 | 0.9601 |
| | | MUR 2 | 128 | 15 | M1 | 0.873 | 0.125 | 0.9978 |
| | | MUR 3 | 214 | 25 | M1 | 0.853 | 0.025 | 0.8781 |
| C02 | 1088 | CAR 1 | 272 | 25 | RC1 | 0.644 | 0.054 | 0.6975 |
| | | CAR 2 | 381 | 35 | RC2 | 0.484 | 0.045 | 0.5285 |
| | | CAR 3 | 272 | 25 | RC2 | 0.484 | 0.015 | 0.4985 |
| | | CAR 4 | 163 | 15 | RC3 | 0.324 | 0.118 | 0.4420 |
| C03 | 67 | CAR 1 | 67 | 100 | RC3 | 0.324 | 0.05 | 0.3740 |
| C04 | 591 | CAR 1 | 177 | 30 | RC2 | 0.484 | 0.052 | 0.5355 |
| | | CAR 2 | 414 | 70 | RC2 | 0.484 | 0.023 | 0.5065 |
| C05 | 161 | CAR 1 | 57 | 35 | RC1 | 0.644 | -0.013 | 0.6315 |
| | | CAR 2 | 32 | 20 | RC1 | 0.644 | 0.053 | 0.6965 |
| | | CAR 3 | 56 | 35 | RC2 | 0.484 | 0.034 | 0.5175 |
| | | CAR 4 | 16 | 10 | RC2 | 0.484 | 0.033 | 0.5175 |
| C06 | 113 | CAR 1 | 45 | 40 | RC3 | 0.324 | -0.013 | 0.3115 |
| | | CAR 2 | 34 | 30 | RC2 | 0.484 | -0.008 | 0.4765 |
| | | CAR 3 | 34 | 30 | RC2 | 0.484 | 0.045 | 0.5285 |
| C07 | 604 | MUR 1 | 121 | 20 | M3 | 0.78 | 0.109 | 0.8885 |
| | | CAR 1 | 181 | 30 | RC1 | 0.644 | 0.055 | 0.6985 |
| | | CAR 2 | 121 | 20 | RC1 | 0.644 | 0.113 | 0.7565 |
| | | CAR 3 | 60 | 10 | RC2 | 0.484 | 0.006 | 0.4900 |
| | | CAR 4 | 121 | 20 | RC1 | 0.644 | 0.1 | 0.7440 |
| C08 | 32 | CAR 1 | 32 | 100 | RC2 | 0.484 | 0.001 | 0.4845 |
| C09 | 181 | CAR 1 | 27 | 15 | RC2 | 0.484 | 0.005 | 0.4886 |
| | | CAR 2 | 45 | 25 | RC2 | 0.484 | 0.095 | 0.5793 |
| | | CAR 3 | 109 | 60 | RC2 | 0.484 | 0.041 | 0.5245 |
| C10 | 96 | MUR 1 | 82 | 85 | M3 | 0.78 | 0.105 | 0.8846 |
| | | MUR 2 | 14 | 15 | M3 | 0.76 | 0.148 | 0.9075 |

## 6.6 Results

This section summarizes the results of the two-stage stochastic model and compares them with the deterministic cost-benefit analysis. Optimal budget allocations were obtained up to 200,000 € for CPE and up to 1–4 million € for VPE. Figure 6a reports the percentage of budget assigned to proactive strengthening (PS) and reactive repair (RR) as a function of the available budget, expressed as a percentage of Budget required for the seismic Retrofitting of All the Buildings (BRAB) (1.614 billion €), calculated from the total surface of the 100 building clusters (388,900 m² for masonry; 2,415,000 m² for RC) and the retrofitting unit costs (424.54 €/m² and 600 €/m², respectively). The curves distinguish the CPE and VPE correlations ($p_k$ =100% for all damage levels in CPE; $p_5$=$p_4$=$p_3$=100%, $p_2$=50%, $p_1$=10% in VPE). Although Table 10 and Table 11 are based on deterministic assumptions, they provide qualitative guidance for interpreting the stochastic outcomes.

For CPE, Figure 6a shows that at low budgets only a small share (~2%) is devoted to strengthening, with most resources allocated to RC repair. As the budget increases, the PS share grows rapidly up to about 6% of BRAB and then more gradually up to around 12%, at which point PS and RR balance. Beyond this threshold, preventive strengthening becomes increasingly advantageous.

Figure 6b confirms this behaviour: under CPE, low budgets are almost entirely allocated to repair; strengthening becomes progressively dominant only beyond ~12% of BRAB. This reflects the fact that, under CPE, reducing evacuees requires transitioning buildings from any damage level to D0. Since few masonry buildings in Patti can be improved from D1→D0 through local strengthening (Table 10), PS remains limited at very low budgets. The first significant actions are repairs of RC and masonry buildings (D1→D0), consistent with the trends in Figure 6b.

Under VPE, the pattern differs because evacuees depend on damage severity. Reducing damage without necessarily reaching D0 is beneficial, so the order of interventions is governed by cost/evacuee efficiency (Table 11). Figure 6b shows that, for budgets up to about 10% of BRAB, all resources are allocated to strengthening; beyond this point, PS remains predominant (about 75%) up to roughly 20% of BRAB.

Figure 7a and Figure 7b report the percentage of buildings receiving seismic retrofitting, seismic improvement, or local strengthening. Under CPE, no strengthening occurs below 1% of BRAB; as the budget increases, local strengthening is applied first, followed by improvement and, at higher budgets, retrofitting. For any given budget, local strengthening is generally the most common intervention. Under VPE, local strengthening dominates at low budgets and increases up to about 6% of BRAB; improvement becomes increasingly relevant and retrofitting is significant only at high budgets (~19.9% of BRAB).

Figure 8a–d separate these results for masonry and RC buildings. For masonry, local strengthening is rarely selected; retrofitting dominates under CPE while improvement is prevalent under VPE. For RC structures, seismic retrofitting is never adopted, and local strengthening remains the primary intervention type in both CPE and VPE.

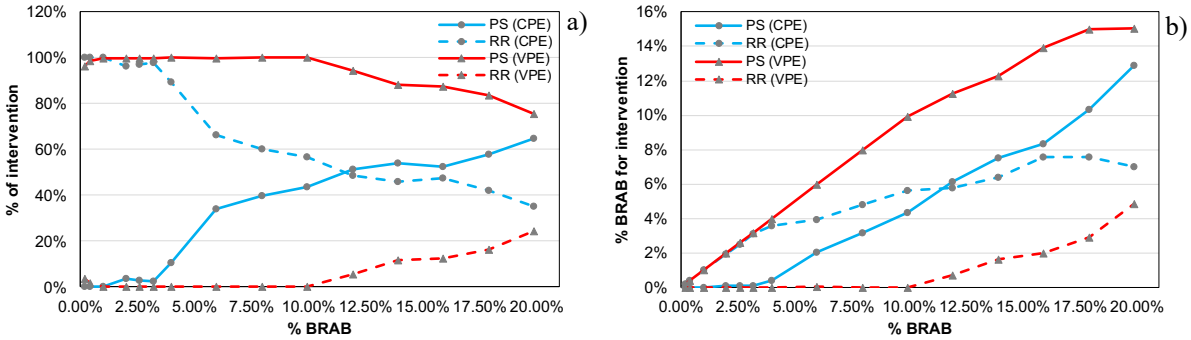


Figure 6: a) and b) Percentage of actual budget allocated for optimized strengthening or repair, in the case of CPE and VPE

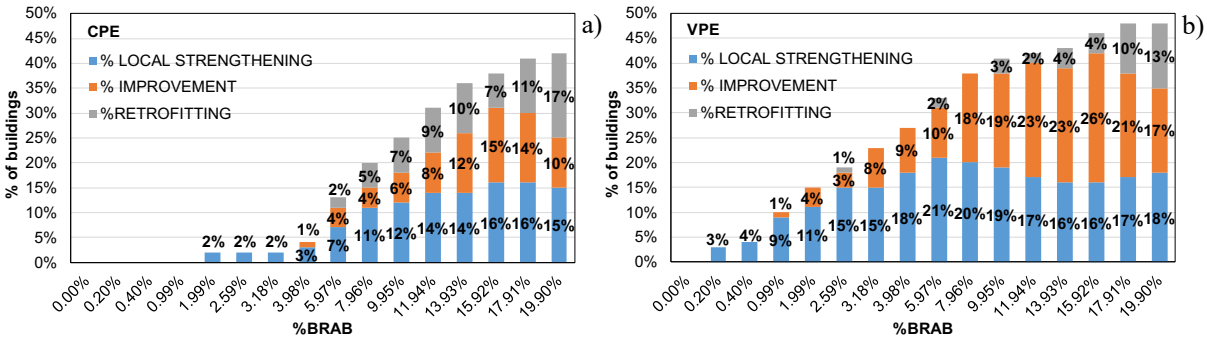


Figure 7: a) and b) Percentage of buildings subjected to strengthening interventions of high, medium and low level, for CPE and VPE, respectively

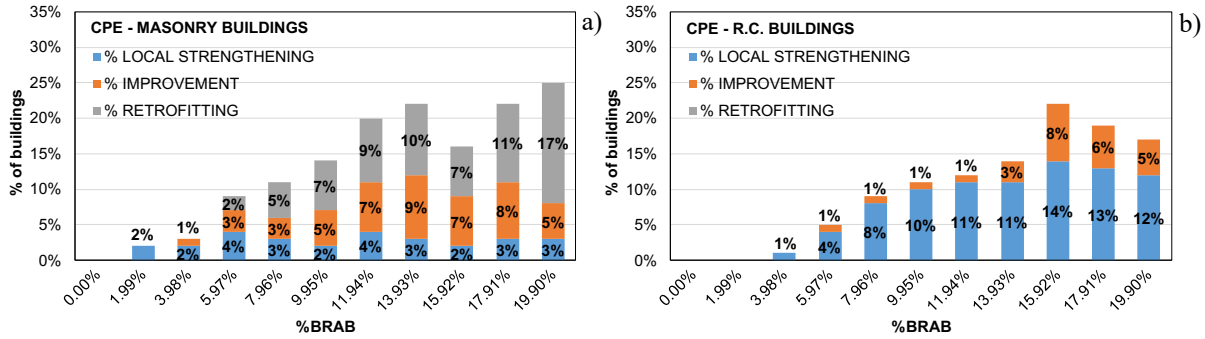

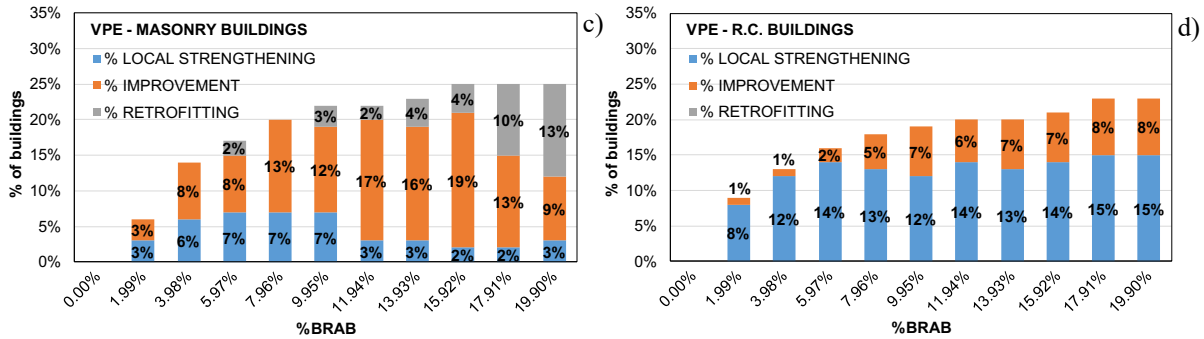


Figure 8: a), b), c) and d) Percentage of masonry and R.C. buildings subjected to strengthening interventions of high, medium and low level, for CPE and VPE, respectively

Figure 9a shows the percentage of evacuees remaining after repair for CPE and VPE as the budget increases. The curves compare the optimized PS+RR allocation (solid lines) with the case where the entire budget is used for RR only (dotted lines). In both cases, the number of evacuees decreases with increasing budget, and PS+RR consistently outperforms RR alone. The grey curves highlight that the benefit of including PS grows as the available budget increases.

Figure 9b (CPE) and 5c (VPE) present the mean damage distribution after PS interventions for different strengthening budgets, expressed as percentages of BRAB, and compare it with the no-strengthening case (0% PS). In both correlations, the share of buildings with no or slight damage (D0–D1) increases with budget, while D2 decreases, particularly under VPE. Severe damage (D3–D5) declines slowly in CPE but is nearly eliminated in VPE, demonstrating the higher effectiveness of the VPE correlation in reducing high damage levels.

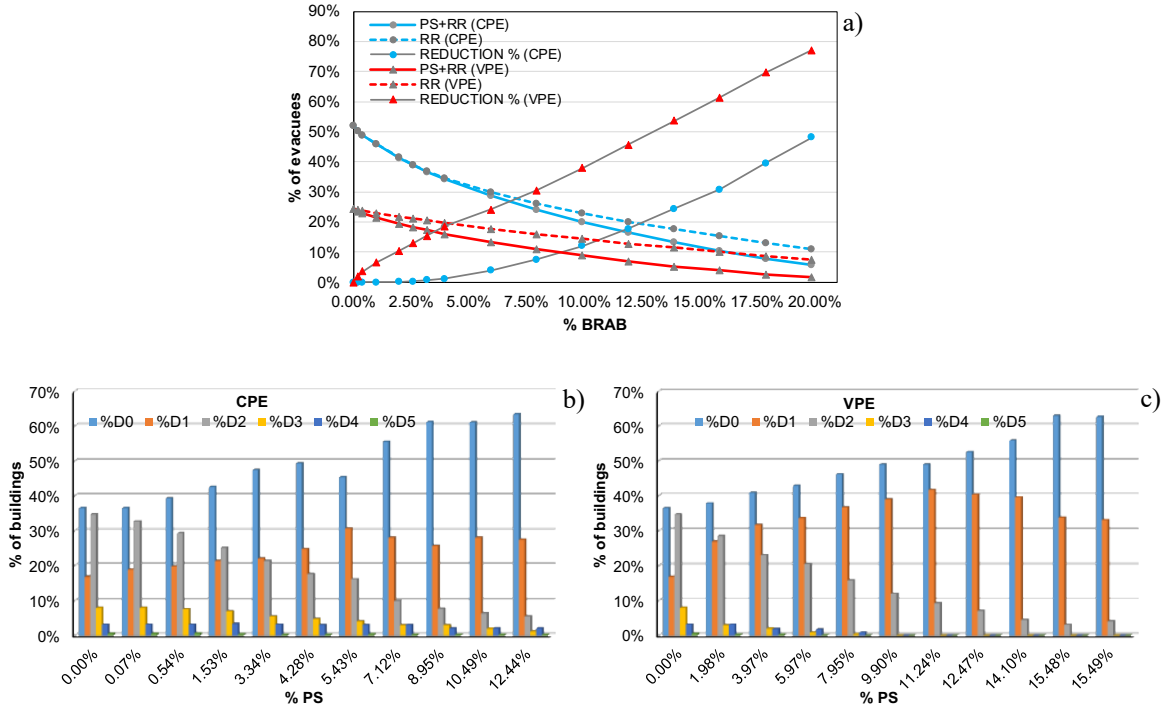


Figure 9: a) Percentage of remaining evacuees for different budgets; Mean damage distributions after proactive strengthening actions in the case of b) CPE and c) VPE

## 6.7. Conclusions

In this task a decision-making strategies for optimally allocating resources between proactive strengthening (PS) of residential buildings and reactive repair (RR) after earthquakes, with the objective of minimizing evacuees—i.e., residents of damaged buildings, has been developed. A two-stage stochastic model with recourse was used, assuming a fixed maximum budget shared between PS and RR.

The model integrates seismic exposure data from the CARTIS survey procedure and evaluates vulnerability using the Heuristic method (masonry) and the Macroseismic method (RC). Intervention costs were derived from literature and recent Italian seismic mitigation policies. Two damage–evacuee correlations were considered: a constant evacuation rate for all damaged buildings (CPE) and a variable one (VPE), where evacuees decrease for lower damage states (D2 and D1). The methodology was applied to a small municipality in western Sicily.

Based on the discussions reported in the previous sections, the following conclusions can be drawn:

- The percentage of evacuees decreases as the intervention budget increases. For any fixed budget, optimized PS+RR allocation yields fewer evacuees than using the entire budget for RR only, in both CPE and VPE.
- Optimal budget allocation is highly sensitive to the assumed correlation between damage level and number of evacuees.
- Regarding PS–RR distribution:
    - Under CPE, low budgets should prioritize RR, with limited strengthening; as budget increases, the share devoted to PS progressively grows, eventually exceeding RR for high budgets.
    - Under VPE, the opposite occurs for low budgets, and for high budgets about 75% of funds should go to PS and 25% to RR.
- Concerning strengthening types:
    - Under CPE, low budgets mainly support local strengthening of a small share of buildings; with higher budgets, all strengthening types increase. Local strengthening remains the most common, followed by improvement and then retrofitting. At 19.9% of BRAB, retrofitting and local strengthening apply to similar building shares, while improvement affects about 35% fewer buildings.
    - Under VPE, local strengthening is again prioritized at low budgets, but both local strengthening and seismic improvement grow rapidly with increasing budget, while retrofitting appears only at higher budgets and in smaller proportions.
- For expected damage distributions after PS, the VPE-based prioritization is more effective, producing a rapid reduction of severe damage (D3–D5) and a steady increase in undamaged/lightly damaged buildings (D0–D1).
- Several simplifying assumptions were necessary for developing the method; therefore, results are not universally generalizable. Local recalibration is required for applications in other contexts. Nonetheless, the proposed framework provides a valid and efficient procedure for resource allocation.

# 7. Development of a multilevel optimization strategy for enhancing seismic safety and energy performance in school building portfolios

## 7.1 Introduction

School buildings play a dual role in society: they are essential for education and also serve as key assets for community resilience during and after disasters (Mutch, 2015; Wang, 2016; Ilumin & Oreta, 2018). However, past earthquakes have repeatedly demonstrated the high vulnerability of school infrastructures, often resulting in severe damage, loss of life, and long-term disruption of social and economic systems (Augenti et al., 2004). These impacts highlight the urgent need for improved seismic risk mitigation strategies.

In seismically active countries such as Italy, significant efforts have been made to assess and reduce the vulnerability of school buildings through national programs, risk assessment tools, and databases such as IRMA and Da.D.O (Faravelli et al., 2023; Dolce et al., 2019). These initiatives have enabled the development of fragility curves and simplified assessment models tailored to the Italian context (Cattari et al., 2024). Nevertheless, several limitations remain.

Existing methodologies often rely on tiered approaches, where simplified screening is followed by more detailed analysis. While efficient, this strategy may overlook critical vulnerabilities, especially in unreinforced masonry (URM) buildings, whose behavior is highly variable and not always consistent with design code assumptions. Moreover, many studies focus primarily on damage assessment and prioritization, with limited attention to the effectiveness of specific retrofit interventions and their integration at the portfolio level (Saler et al., 2023; Caterino et al., 2018).

Another major gap lies in the lack of holistic cost-benefit evaluation and the limited integration of multiple objectives such as safety, cost, and feasibility. Additionally, the growing importance of energy efficiency and climate-related considerations has further increased the complexity of decision-making in infrastructure management (Marini et al, 2022; Manfredi et al., 2018).

To address these challenges, in the contest of Task 7.3, a multi-level, portfolio-based decision-making framework that integrates seismic safety, cost-effectiveness, and implementation feasibility was developed (FathiAzar & Cattari, 2025). The approach emphasizes life safety as a non-negotiable requirement and introduces a multi-objective optimization strategy to support intervention planning across large building portfolios.

## 7.2 Methodology

### 7.2.1 Conceptual Framework and Scale

The proposed methodology operates at the **portfolio level**, bridging the gap between building-scale detailed analyses and territorial-scale risk assessments. This intermediate scale allows for both contextual sensitivity and computational efficiency, making it suitable for managing heterogeneous building stocks with incomplete data .

- The framework consists of three main stages:
- Collaborative and contextual decision-making
- Safety-focused intervention selection
- Evolutionary multi-objective optimization

These stages are interconnected and allow for iterative refinement of decisions.

### 7.2.2 Decision Variables and Risk Metrics

A key component of the methodology is the identification of **decision variables (DVs)** through stakeholder engagement and data analysis. These variables include:

- Structural safety (Safety Index at Life Safety – SI-LS)
- Expected Annual Loss (EAL)
- Cost, payback period (PP), and realization time

Both conditional and unconditional risk metrics are used, combining event-based analysis with probabilistic assessment (Dolce, 2021; Yoshikawa & Goda, 2014). The SI-LS is adopted as the primary safety indicator, defined as the ratio between structural capacity and seismic demand. A threshold value of SI-LS = 1 is used to identify buildings requiring intervention, ensuring that life safety remains the dominant objective.

### 7.2.3 Safety-Oriented Intervention Selection

The second stage focuses on identifying retrofit strategies capable of improving structural safety.

Initially, buildings are classified using fragility curves, derived from validated models such as DBV-Masonry (Cattari et al., 2021). These curves represent the probability of reaching different damage states under seismic loading.

For buildings with insufficient safety levels, a set of potential retrofit interventions is defined based on:

- Structural characteristics
- Construction period
- Observed vulnerabilities

These interventions include both individual techniques (e.g., injections, tie rods, diaphragm strengthening) and combined solutions. Each intervention is evaluated by recalculating fragility curves and verifying whether the SI-LS threshold is achieved. Only effective strategies are retained for further analysis.

### 7.2.4 Evolutionary Multi-Objective Optimization

The final stage employs a Genetic Algorithm (GA) to optimize intervention strategies across the portfolio.

Each solution represents a combination of retrofit actions applied to all buildings. The optimization simultaneously minimizes:

- Total cost
- Payback period
- Realization time

Pareto-optimal solutions are identified, representing trade-offs between competing objectives. To support decision-making, the Analytic Hierarchy Process (AHP) is used to assign weights to decision variables based on expert judgment (Andreolli et al., 2021). This approach ensures that final decisions reflect both technical performance and stakeholder priorities.

### 7.2.5 Integration of Energy Efficiency

The framework also considers the integration of energy retrofit measures, although these are analyzed separately due to data limitations and differences in economic dynamics.

Simplified models are used to estimate energy consumption and savings (Ademovic et al, 2022, Pohoryles et al., 2022; Passoni et al., 2024), highlighting the challenges of combining seismic and energy interventions at the portfolio scale.

## 7.3 Case Study

The methodology is applied to a portfolio of **85 URM school buildings** located in the Friuli-Venezia Giulia (FVG) region in northeastern Italy . The dataset includes detailed information on:

- Construction period
- Building geometry
- Number of stories
- Material properties

The majority of buildings were constructed before the introduction of modern seismic design codes, making them particularly vulnerable.

Seismic demand is defined using the Italian hazard model (NTC18), with site-specific parameters such as VS30 values and return periods corresponding to different limit states.

The DBV-Masonry model is used to generate fragility curves for both as-built and retrofitted conditions. The model has been validated through numerical simulations and empirical data, demonstrating good agreement with more advanced approaches (Giusto et al., 2025).

A set of retrofit strategies is defined, including five individual methods (M1–M5) and four combined intervention packages (P1–P4), targeting different vulnerability mechanisms. of different methods. Specifically, five single intervention methods (M1 to M5) and four intervention packages (P1 to P4) are evaluated. The single intervention methods include: M1: Injection, M2: Overlay, M3: Tie, M4: Diaphragm Improvement, and M5: Ring Beam. The intervention packages are as follows: P1: Injection +Diaphragm Improvement, P2: Injection +Tie, P3: Overlay +Diaphragm Improvement, and P4: Overlay +Tie.

## 7.4 Results

The application of the proposed framework to a portfolio of 85 unreinforced masonry school buildings in Friuli-Venezia Giulia highlights a pronounced variability in seismic performance. The Safety Index at Life Safety (SI-LS) shows an average value of 0.85 (range: 0.50–1.86), while the Expected Annual Loss (EAL) averages 1.12% (range: 0.41–2.83%). As a consequence, 66 buildings require retrofit interventions to meet the adopted safety threshold (SI-LS = 1), confirming the widespread vulnerability of the analyzed stock.

The analysis reveals consistent relationships between structural characteristics and performance. Buildings with fewer stories and smaller footprint areas generally exhibit higher safety levels, whereas older constructions—especially pre-19th century—show significantly lower SI-LS values. Statistical analysis confirms that the number of stories is the most influential parameter affecting both SI-LS and EAL, while footprint area primarily affects economic losses. These findings support the use of simplified indicators for portfolio-level prioritization, although their generalization requires caution.

The evaluation of retrofit strategies shows that economic efficiency strongly depends on the initial structural condition. Buildings close to the safety threshold require only minor upgrades, which lead to limited reductions in EAL and consequently long payback periods. In contrast, more vulnerable buildings allow greater risk reduction, although the requirement to reach SI-LS = 1 may still result in extended payback times. The results also indicate that intervention effectiveness varies with building typology: lightweight measures such as tie rods are most efficient for moderately deficient structures, whereas more complex solutions—such as overlay combined with diaphragm strengthening—are often necessary for highly vulnerable or taller buildings.

The optimization process identifies a portfolio-wide intervention scenario capable of ensuring compliance with safety targets while balancing cost, realization time, and payback period. The selected solution achieves full compliance for all buildings with a total investment of approximately €15.61 million (average €135/m²), although a limited number of structures require advanced interventions. The results also confirm that older buildings provide higher safety gains per unit of investment, reinforcing their prioritization.

The analysis of energy retrofit measures, performed separately, indicates that most standalone interventions are characterized by long payback periods, often exceeding 50 years. Even with financial incentives, only a limited number of measures—such as building envelope insulation—show acceptable economic performance. Overall, the findings highlight the limited financial viability of isolated energy retrofits and suggest that integrated seismic-energy strategies offer a more effective approach.

## 7.5 Conclusions

The study demonstrates the effectiveness of a multi-level, portfolio-based framework for the prioritization of seismic retrofit interventions in school buildings, emphasizing safety as a non-negotiable constraint. The results confirm that seismic risk and retrofit efficiency are strongly influenced by building characteristics, particularly structural vulnerability and height, and that older buildings represent the most cost-effective targets for intervention.

The findings also highlight the limitations of standalone energy retrofits, which generally exhibit weak economic performance, reinforcing the need for integrated seismic and energy upgrading strategies. By combining probabilistic risk assessment, performance-based metrics, and multi-objective optimization, the proposed approach supports more informed and strategic decision-making at the infrastructure portfolio level.

Future developments should focus on improving data availability, integrating environmental indicators, and explicitly addressing uncertainty in order to enhance the robustness and applicability of the framework in real-world planning contexts.

# 8. General Conclusions

Task 3.7.3 aimed to develop a comprehensive and operational framework for the optimal selection of mitigation and adaptation strategies in multi-risk contexts, integrating methodological advancements, modelling approaches, and application-oriented tools across different spatial and decision scales.

A first key contribution of the work lies in the transition from indicator-based assessment to decision-support systems. Starting from the Essential Resilience Indicators (ERI) framework developed in previous tasks, the research has demonstrated how resilience metrics can be transformed into operational tools for strategy selection. By linking indicators to action domains and organizing them into coping, adaptive, and transformative capacities, the framework provides a structured bridge between the analytical evaluation of resilience and the implementation of concrete interventions. This represents a significant step forward in overcoming the traditional gap between assessment and decision-making in disaster risk reduction.

This conceptual advancement is further strengthened through the integration of a Multi-Criteria Decision Analysis (MCDA) approach. By assigning weights to indicators through participatory methods and combining them with scenario-based performance evaluations, the proposed framework allows for the explicit comparison of alternative strategies, taking into account trade-offs between short-term effectiveness, long-term sustainability, and social inclusiveness. The integration with GIS-based tools and risk modelling enhances the spatial and dynamic dimension of the analysis, supporting more transparent and informed decision processes.

At the infrastructure scale, the development of a life-cycle, multi-objective prioritization framework for bridge networks highlights the importance of considering interacting hazards, climate change effects, and deterioration processes. By combining probabilistic fragility models, network functionality metrics, recovery modelling, and socio-economic indicators, the approach enables a comprehensive assessment of system performance and supports the identification of cost-effective and resilience-oriented intervention strategies.

At the urban scale, the proposed stochastic model for budget allocation between proactive strengthening and reactive repair provides an innovative contribution to seismic risk mitigation. By explicitly accounting for uncertainty and linking pre-event interventions with post-event consequences, the model demonstrates how optimized resource allocation can significantly reduce the number of evacuees. The results underline the importance of integrating preventive and reactive strategies and show that their optimal balance depends strongly on the assumed relationship between damage and social impact.

At the building portfolio scale, the multilevel optimization framework for school buildings further extends the decision-support approach by integrating seismic safety, economic performance, and implementation constraints. The results confirm that vulnerability reduction strategies must be tailored to building characteristics and that prioritization should focus on structures with the highest potential for risk reduction. At the same time, the analysis highlights the limited effectiveness of standalone energy retrofit measures, emphasizing the need for integrated seismic–energy strategies.

Overall, the deliverable demonstrates that resilience in multi-risk contexts is a systemic and multi-dimensional property that cannot be addressed through isolated measures. Instead, it requires integrated approaches that combine:

- quantitative modelling and qualitative assessment,
- short-term response and long-term transformation,
- infrastructure, buildings, and governance dimensions.

The performed studies has investigated possible pathways from resilience assessment to strategy selection, supporting the development of more effective, adaptive, and sustainable risk reduction policies.

# 8. References


Ademovic, N., Formisano, A., Penazzato, L., & Oliveira, D. V. (2022). Seismic and energy integrated retrofit of buildings: A critical review. Frontiers in Built Environment, 8, 963337. https://doi.org/10.3389/fbuil.2022.963337

Andreolli, F., Bragolusi, P., D'Alpaos, C., Faleschini, F., & Zanini, M. A. (2022). An AHP model for multiple-criteria prioritization of seismic retrofit solutions in gravity-designed industrial buildings. Journal of Building Engineering, 45, 103493. https://doi.org/10.1016/j.jobe.2021.103493

Argyroudis, S. A., Mitoulis, S. A., Hofer, L., Zanini, M. A., Tubaldi, E., & Frangopol, D. M. (2020). Resilience assessment framework for critical infrastructure in a multi-hazard environment: Case study on transport assets. Science of the Total Environment, 714, 136854.

Augenti, N., Cosenza, E., Dolce, M., Manfredi, G., Masi, A., & Samela, L. (2004). Performance of school buildings during the 2002 Molise, Italy, earthquake. Earthquake Spectra, 20, 257–270. https://doi.org/10.1193/1.1769374

Bruneau, M., Chang, S. E., Eguchi, R. T., Lee, G. C., O'Rourke, T. D., Reinhorn, A. M., Shinozuka, M., Tierney, K., Wallace, W. A., & von Winterfeldt, D. (2003). A framework to quantitatively assess and enhance the seismic resilience of communities. Earthquake Spectra, 19(4), 733–752.

Cacace, F., Zuccaro, G., De Gregorio, D., & Perelli, F. L. (2018). Building inventory at national scale by evaluation of seismic vulnerability classes distribution based on census data analysis: BINC procedure. International Journal of Disaster Risk Reduction, 28, 384–393. https://doi.org/10.1016/j.ijdrr.2018.03.016

Capacci, L., Biondini, F., & Frangopol, D. M. (2022). Resilience of aging structures and infrastructure systems with emphasis on seismic resilience of bridges and road networks: Review. Resilient Cities and Structures, 1(2), 23–41.

Caterino, N., Azmoodeh, B. M., & Manfredi, G. (2018). Seismic risk mitigation for reinforced concrete frame buildings through optimal allocation of a limited budget. Advances in Civil Engineering, 2018, 1–18. https://doi.org/10.1155/2018/8184756

Cattari, S., Alfano, S., Manfredi, V., Borzi, B., Faravelli, M., Di Meo, A., da Porto, F., Saler, E., Dall'Asta, A., Gioiella, L., Di Ludovico, M., Del Vecchio, C., Del Gaudio, C., Verderame, G., Gattesco, N., Boem, I., Speranza, E., Dolce, M., Lagomarsino, S., & Masi, A. (2024). National risk assessment of Italian school buildings: The MARS project experience. International Journal of Disaster Risk Reduction, 113, 104822. https://doi.org/10.1016/j.ijdrr.2024.104822

Colajanni, P., & D'Anna, J. (2023). Seismic risk assessment of residential buildings by the heuristic vulnerability model: Influence of fragility curve models and inventory scale. Bulletin of Earthquake Engineering. https://doi.org/10.1007/s10518-023-01801-z

Colajanni, P., Cucchiara, C., D'Anna, J., Pennisi, S., & Pagnotta, S. (2023). Vulnerability and seismic exposure of residential building stock in the historic center of Alcamo. Applied Sciences, 13(12), 7092.

DPCI. (2021). Ordinanza n. 780 del 20 maggio 2021. Dipartimento della Protezione Civile.

Di Ludovico, M., De Martino, G., Manfredi, V., Masi, A., Prota, A., Sorrentino, L., & Zucconi, M. (2023). Loss functions for the risk assessment of residential buildings. Buildings, 13(11), 2817.

Di Ludovico, M., De Martino, G., Prota, A., Manfredi, G., & Dolce, M. (2022). Relationships between empirical damage and direct/indirect costs for the assessment of seismic loss scenarios. Bulletin of Earthquake Engineering.

Dolce, M., Prota, A., Borzi, B., da Porto, F., Lagomarsino, S., Magenes, G., Moroni, C., Penna, A., Polese, M., & Speranza, E. (2021). Seismic risk assessment of residential buildings in Italy. Bulletin of Earthquake Engineering, 19, 2999–3032.

Dolce, M., Prota, A., Borzi, B., da Porto, F., Lagomarsino, S., Magenes, G., Moroni, C., Penna, A., Polese, M., & Speranza, E. (2021). Seismic risk assessment of residential buildings in Italy. Bulletin of Earthquake Engineering, 19, 2999–3032.

Dolce, M., Speranza, E., Giordano, F., Borzi, B., Bocchi, F., Conte, C., Di Meo, A., Faravelli, M., & Pascale, V. (2019). Observed damage database of past Italian earthquakes: The Da.D.O. WebGIS. Bollettino di Geofisica Teorica ed Applicata, 60, 141–164. https://doi.org/10.4430/bgta0254

FEMA. (1994). Typical costs for seismic rehabilitation of existing buildings (FEMA-156).

Faravelli, M., Borzi, B., Onida, M., Cattari, S., Alfano, S., Masi, A., Manfredi, V., & Lagomarsino, S. (2023). An Italian platform for seismic risk assessment of school buildings. Procedia Structural Integrity, 44, 107–114. https://doi.org/10.1016/j.prostr.2023.01.015

FathiAzar, A., & Cattari, S. (2025). Multilevel optimization strategy for enhancing seismic safety and energy performance in school building portfolios. International Journal of Disaster Risk Reduction, 130, 105822. https://doi.org/10.1016/j.ijdrr.2025.105822

Figueira, J., & Roy, B. (2002). Determining the weights of criteria in the ELECTRE type methods with a revised Simos' procedure. European Journal of Operational Research, 139(2), 317–326.

Follador, V., Donà, M., Carpanese, P., Saler, E., D'Alpaos, C., & da Porto, F. (2024). Seismic retrofit cost model for Italian masonry residential buildings. International Journal of Disaster Risk Reduction, 105, 104373.

Fung, J. F., Sattar, S., Butry, D. T., & McCabe, S. L. (2021). The total costs of seismic retrofits: State of the art. Earthquake Spectra, 37(4), 2991–3014.

Giusto, S., Boem, I., Alfano, S., Gattesco, N., & Cattari, S. (2025). Derivation of seismic fragility curves through mechanical-analytical approaches. Bulletin of Earthquake Engineering, 23, 2611–2646. https://doi.org/10.1007/s10518-025-02137-6

Gkournelos, P. D., Triantafillou, T. C., & Bournas, D. A. (2021). Seismic upgrading of existing reinforced concrete buildings: A state-of-the-art review. Engineering Structures, 240, 112273.

Gkournelos, P. D., Triantafillou, T. C., & Bournas, D. A. (2022). Seismic upgrading of existing masonry structures: A state-of-the-art review. Soil Dynamics and Earthquake Engineering, 161, 107428.

Grünthal, G. (1998). European macroseismic scale 1998 (EMS-98).

Ilumin, R. C., & Oreta, A. W. C. (2018). A post-disaster functional asset value index for school buildings. Procedia Engineering, 212, 230–237. https://doi.org/10.1016/j.proeng.2018.01.030

Jafari, L., & Biondini, F. (2025). Multi-objective resilience-based optimal prioritization of aging bridge networks under multiple hazards in a changing climate. Structure and Infrastructure Engineering (in press).

Jafari, L., Capacci, L., Biondini, F., & Khanmohammadi, M. (2023). Resilience-based optimal management of aging bridge networks under mainshock-aftershock sequences. In F. Biondini & D. M. Frangopol (Eds.), Life-cycle of structures and infrastructure systems (pp. 1869–1876). CRC Press.

Jafari, L., Khanmohammadi, M., Capacci, L., & Biondini, F. (2024). Resilience-based optimal seismic retrofit and recovery strategies of bridge networks under mainshock-aftershocks sequences. Journal of Infrastructure Systems, 30(3), 04024015. https://doi.org/10.1061/JITSE4.ISENG-2301

Jafarzadeh, R., Ingham, J. M., Wilkinson, S., González, V., & Aghakouchak, A. A. (2014b). Artificial neural network for retrofit cost prediction. Journal of Construction Engineering and Management, 140(2), 04013044.

Jafarzadeh, R., Wilkinson, S., González, V., Ingham, J. M., & Amiri, G. G. (2014a). Predicting seismic retrofit construction cost. Journal of Construction Engineering and Management, 140(3), 04013062.

Lagomarsino, S., & Giovinazzi, S. (2006). Macroseismic and mechanical models. Bulletin of Earthquake Engineering, 4, 415–443.

Lagomarsino, S., Cattari, S., & Ottonelli, D. (2021). The heuristic vulnerability model. Bulletin of Earthquake Engineering, 19, 3129–3163.

MIT. (2018). Norme tecniche per le costruzioni (NTC18).

Maio, R., Estêvão, J. M., Ferreira, T. M., & Vicente, R. (2020). Cost-benefit analysis of seismic retrofitting strategies. Engineering Structures, 206, 110050.

Manfredi, V., & Masi, A. (2018). Seismic strengthening and energy efficiency. Buildings, 8, 36. https://doi.org/10.3390/buildings8030036

Mannella, A., Di Ludovico, M., Sabino, A., Prota, A., Dolce, M., & Manfredi, G. (2017). Analysis of population assistance. Sustainability, 9(8), 1395.

Marini, A., Passoni, C., Belleri, A., Feroldi, F., Preti, M., Metelli, G., Riva, P., Giuriani, E., & Plizzari, G. (2022). Combining seismic retrofit with energy refurbishment. European Journal of Environmental and Civil Engineering, 26, 2475–2495. https://doi.org/10.1080/19648189.2017.1363665

Marques, R., Lamego, P., Lourenço, P. B., & Sousa, M. L. (2018). Efficiency of seismic strengthening techniques. Journal of Earthquake Engineering, 22(9), 1590–1625.

Milić, P., & Kušter Marić, M. (2023). Climate change effect on durability of bridges and other infrastructure. Građevinar, 75(9), 896–906.

Mutch, C. (2015). The role of schools in disaster settings. International Journal of Educational Development, 41, 283–291. https://doi.org/10.1016/j.ijedudev.2014.06.008

Nasr, A., Kjellstrom, E., Bjornsson, I., Honfi, D., Ivanov, O. L., & Johansson, J. (2020). Bridges in a changing climate: A study of the potential impacts of climate change on bridges and their possible adaptations. Structure and Infrastructure Engineering, 16(4), 738–749.

Nasrazadani, H., Mahsuli, M., Talebiyan, H., & Kashani, H. (2017). Probabilistic modeling of retrofit cost. Journal of Construction Engineering and Management, 143(8), 04017055.

Nava, G. V., Capacci, L., Biondini, F., & Casti, L. (2023). Life-cycle structural reliability of RC bridge piers under corrosion in a changing climate. In Life-cycle of structures and infrastructure systems (pp. 1625–1633). CRC Press.

Nuzzo, I., Caterino, N., Novellino, A., & Occhiuzzi, A. (2021). Decision making for seismic risk mitigation. Applied Sciences, 11(12), 5539.

Passoni, C., Caruso, M., Felicioni, L., & Negro, P. (2024). The evolution of sustainable renovation of existing buildings. Bulletin of Earthquake Engineering. https://doi.org/10.1007/s10518-024-01991-0

Pohoryles, D. A., Bournas, D. A., da Porto, F., Caprino, A., Santarsiero, G., & Triantafillou, T. (2022). Integrated seismic and energy retrofitting of buildings. Journal of Building Engineering, 61, 105274. https://doi.org/10.1016/j.jobe.2022.105274

Safaeian Hamzehkolaei, N., & Alizamir, M. (2021). Machine learning for retrofit cost estimation. Journal of Soft Computing in Civil Engineering, 5(3), 32–57.

Saler, E., Gattesco, N., & da Porto, F. (2023). A combined approach to prioritise seismic retrofit interventions. International Journal of Disaster Risk Reduction, 93, 103767. https://doi.org/10.1016/j.ijdrr.2023.103767

Turchi, A., Lumino, R., Gambardella, D., & Leone, M. F. (2023). Coping capacity, adaptive capacity, and transformative capacity. Sustainability, 15(14), 10877.

Vona, M., Anelli, A., Mastroberti, M., Murgante, B., & Santa Cruz, S. (2017). Prioritization strategies to reduce seismic risk. Disaster Advances, 10(4), 1–15.

Wang, J.-J. (2016). Study on school-based disaster management. International Journal of Disaster Risk Reduction, 19, 224–234. https://doi.org/10.1016/j.ijdrr.2016.08.005

Yoshikawa, H., & Goda, K. (2014). Financial seismic risk analysis of building portfolios. Natural Hazards Review, 15, 112–120. https://doi.org/10.1061/(ASCE)NH.1527-6996.0000129

Zuccaro, G, (2004). Inventory and Vulnerability of the Residential Building Stock of the National Territory, Risk Maps and Socio-Economic Losses; I.N.G.V./G.N.D.T. - National Institute of Geophysics and Vulcanology/National Group for Earthquake Defense: L'Aquila, Italy, 2004. (In Italian)

Zuccaro, G., Dolce, M., De Gregorio, D., Speranza, E. & Moroni, C. (2015). La scheda CARTIS per la caratterizzazione tipologico-strutturale dei comparti urbani costituiti da edifici ordinari. Valutazione dell'esposizione in analisi di rischio sismico (The CARTIS form for the typological-structural characterization of urban areas with ordinary buildings. Exposure assessment in seismic risk analysis). Proceedings of the 34th National Conference GNGTS, Trieste, Italy, 17–19 November 2015; pp. 281–287. (In Italian).